CHEMICAL AND MECHANICAL CONTROL OF LIESEGANG PATTERNS IN POLYACRYLAMIDE HYDROGELS

A THESIS SUBMITTED TO

THE GRADUATE SCHOOL OF ENGINEERING AND SCIENCE

OF BILKENT UNIVERSITY

IN PARTIAL FULFILLMENT OF THE REQUIREMENTS FOR

THE DEGREE OF

MASTER OF SCIENCE

IN CHEMISTRY

By

Rahym ASHIROV

July 2018

CHEMICAL AND MECHANICAL CONTROL OF LIESEGANG PATTERNS IN POLYACRYLAMIDE HYDROGELS

By Rahym ASHIROV

July 2018

We certify that we have read thesis and that in our opinion it is fully adequate, in scope and in quality, as a thesis for the degree of Master of Science.

_____

Bilge BAYTEKİN (Advisor)

_____

Ferdi KARADAŞ

_____

İrem Erel GÖKTEPE

Approved for the Graduate School of Engineering and Science:

_____

Ezhan KARAŞAN

Director the Graduate School

ABSTRACT

CHEMICAL AND MECHANICAL CONTROL OF LIESEGANG PATTERNS IN POLYACRYLAMIDE HYDROGELS

Rahym ASHIROV

M.S. in Chemistry

Advisor: Bilge Baytekin

July 2018

Self-assembly of molecular components have attracted attention of scientific community in the past decades because of their great potential in designing functional devices in material science. Formed by simultaneous diffusion and precipitation reaction of co-precipitating chemicals in gel media, Liesegang patterns (LPs) are one of the examples of spontaneous pattern formation. LPs have been an attractive topic since their discovery in 1896, due to their wide occurrence in nature and potential applications in sensors, surface sciences, MEMS, bioengineering and microfluidics and fabrication of microstructured materials. Yet, mystery behind formation mechanism of LPs has not been completely solved. More parameters and conditions are needed to be investigated to understand the mechanism.

In this study, we show that formation of Liesegang patterns in polyacrylamide hydrogels can be chemically and mechanically controlled. Firstly, we changed the chemical composition of the hydrogels and monitored the changes in the LPs formed at different locations. Then, we demonstrated that mechanical stress can alter LP formation both in terms of geometry of the rings and of their 'appearance times'. Without any mechanical input, in (pseudo-) 2D gels, LPs form in circular shape. However, when mechanical stress is applied on gels, LPs appear as concentric ovals, the aspect ratio of which increases as applied mechanical stress increases.

In this thesis, for the first time in the literature, we have provided mechanical manipulation of LPs. The time-dependent formation of the patterns and their significant alteration by mechanical input can help us build elastic deformation sensor through the visible patterns.

Keywords: *Liesegang patterns, precipitation patterns, reaction-diffusion systems, stretchable hydrogels, elastic deformation sensors*

ÖZET

POLİAKRİLAMİT HİDROJELLERDE LİESEGANG DESENLERİNİN KİMYASAL VE MEKANİK KONTROLÜ

Rahym ASHIROV

Kimya, Yüksek Lisans

Tez danışmanı: Bilge Baytekin

Temmuz 2018

Moleküler ölçekte kendi kendiliğine düzen oluşumu (self-assembly) fonksiyonel malzemeleri tasarlamamıza olanak verdiği için geçtiğimiz yıllardan beri bilim dünyasının ilgisini çekmeye devam etmektedir. Jel ortamında, birbiriyle etkileşiminde çökelek oluşturan maddelerin eşzamanlı difüzyon ve çökelme reaksiyonu gerçekleştirmesiyle oluşan Liesegang desenleri (LD) kendi kendiliğine desen oluşumunun örneklerinden biridir. Liesegang desenleri 1896 yılında keşfedilmesinden beri, gerek doğada çokça rastlanmasından dolayı, gerekse sensör tasarımında, yüzey bilimlerinde, mikroelektronik mekanik sistemlerinde, biomühendislik ve mikroakışkan alanlarında ve mikroyapılı malzeme üretimi gibi değişik alanlarda olası uygulamalarından ötürü ilgi odağı olmaya devam etmektedir. Yine de, Liesegang desenlerinin nasıl oluştuğunun sırrı hala tam olarak açıklanabilmiş değil. Oluşma mekanizmasını daha iyi anlayabilmemiz için daha fazla etkenlerin ve farklı koşulların araştırılması gerekiyor.

Bu çalışmada, biz Liesegang desenlerinin poliakrilamid hidrojellerinde kimyasal ve mekanik olarak kontrol edilebileceğini gösterdik. Öncelikle, jellerdeki kimyasal içeriğin değişmesiyle Liesegang desenlerindeki değişmeyi gözlemledik ve LD'nin farklı konumlarda oluştuğunu gördük. Sonrasında ise, mekanik gerilimin Liesegang desen oluşumunu hem geometrik olarak hem de oluşma sıklığı yönünden değiştirdiğini ortaya koyduk. Mekanik gerilim uygulanmadığında, yalancı (pseudo) 2 boyutlu jellerde Liesegang desenleri halkasal olarak oluşur. Halbuki, jellere mekanik gerilim uyguladığımızda halkasal desenler oval şekiller olarak meydana geldi. Desenlerin boy-en oranı mekanik gerilimi arttırdıkça yükseldi.

Bu tezde, literatürde ilk defa çökelme desenlerinin mekanik gerilimle kontrol edilebileceğini gösterdik. Zamana bağlı oluşumu ve desenlerin mekanik girdiyle büyük ölçüde değişebilirliği sayesinde, çıplak gözle görülebilir şekilleri kullanarak elastik deformasyon sensörü üretebilmemiz mümkün olacaktır.

Anahtar kelimeler: *Liesegang desenleri, çökelme desenleri, reaksiyon-difüzyon sistemleri, esnetilebilir hidrojeller, elastik deformasyon sensörü*

Acknowledgements

Firstly, I want to express my sincere gratitude to my supervisor Assoc. Prof. Bilge Baytekin for her kind support, guidance and tolerance in my academic life and for being gentle and friendly towards us as her students. I also thank Assoc. Prof. István Lagzi for teaching me a lot about reaction-diffusion systems and being such a nice host in my stay in Hungary. Also, Assoc. Prof. Tarık Baytekin helped me a lot in this project and I thank warmly for his support.

I would like to thank to my colleagues, Mohammad Morsali, for being such a nice friend and project teammate; Atakan Arda Nalbant, for his one year support in my project; Doruk Cezan, for sharing his experiences, whenever I needed and helping to develop experimental setups, and other former and present members of the lab for supporting and motivating me including Tutku Bedük, Özge Bayrak, Ahmet Köseoğlu, Joanna Yiğitbaşı, Fatma Demir, Mertcan Özel, Turab Khan, Meltem Erkan and Merve Saylam.

Furthermore, I am grateful to the examining committee members, Asst. Prof. Ferdi Karadaş and Assoc. Prof. İrem Erel, for their time and help. I would to like to also acknowledge TÜBİTAK for the financial support under project no: 116Z116.

Lastly but the most importantly, I am very thankful to my parents, Yazgylych and Nazik, and to my siblings, Muhammet, Azym, Gülnar and Jemal for their endless support and providing me very happy and warm family environment, which is the reason of any success I would achieve in my life.

TABLE OF CONTENTS

LIST OF TABLES

LIST OF FIGURES

CHAPTER 1

1 INTRODUCTION

1.1. Liesegang Patterns

1.1.1. General information

Precipitation reactions generally form in a disorganised manner and in general products at macroscopic lengths form [1]. Nevertheless, simultaneous diffusion and precipitation reaction of co-precipitating chemicals in gel media may lead to organized material and complex patterns formed through self-assembly [2]. Periodic precipitations, also known as Liesegang patterns (LPs) discovered by Raphael Edward Liesegang in 1896 [3], are one of the important examples of such precipitations, in which organized structures formed in reaction-diffusion systems. Although the mechanism of formation of Liesegang patterns is still not very clear, the procedure is quite straightforward: An aqueous solution of “outer” electrolyte is let to diffuse into a gel containing a co-precipitating “inner” electrolyte, where the precipitation/diffusion events leads to the LP patterns. These patterns can be formed in different dimensions: bands in one dimension, rings in two dimensions, or shells in three dimensions [4, 5]. Since the formation procedure of Liesegang pattern is easy, so far many empirical attempts provided LPs with different cations, anions, and the mostly available gels such as gelatin and agarose. In Figure 1, precipitation bands formed in one dimension are illustrated for different sparingly soluble salts. In Table 1, some of the most common systems used for investigation of Liesegang phenomenon is presented. Liesegang patterns widely occur in nature, too (Figure 2), especially in rock formation [6].

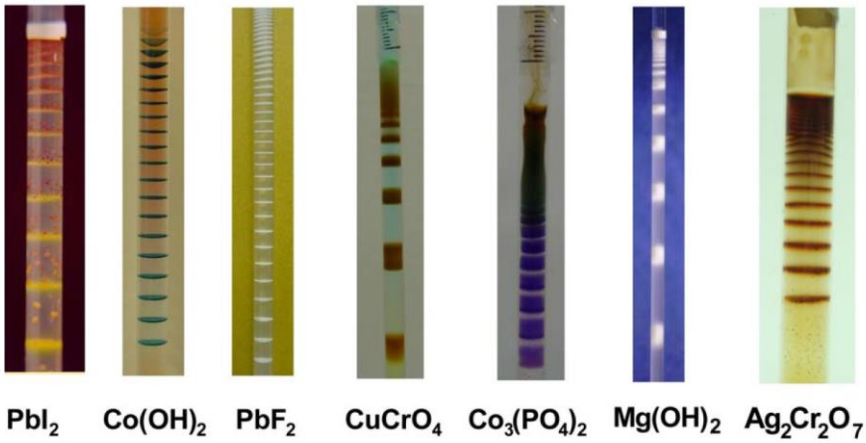

Figure 1. Liesegang band patterns in gels, for a number of sparingly soluble salts [1]

Mobile Phase (Outer Electrode)	**Stationary Phase (Gel – Possible Inner Electrodes)**
NH_3	Gelatin – $CoCl_2$; $MgCl_2$; $MnCl_2$; $UO_2(NO_3)_2$
NaOH	Gelatin – $MgCl_2$; $UO_2(NO_3)_2$; $CoCl_2$
$AgNO_3$	Gelatin – $CuSO_4$; $UO_2(NO_3)_2$; K_2CrO_4; $K_2Cr_2O_7$
$CuCl_2$	Agarose – K_2CrO_4
NH_4OH	Agarose – $CoCl_2$
$Pb(NO_3)_2$	Gelatin – KI
Liesegang Rings with Nanoparticle Precipitates	
AuMUA	Agarose – AuTMA
AgMUA	Agarose – AgTMA

Table 1. Some of the most common systems for investigation of the Liesegang phenomenon

Figure 2. Liesegang patterns in nature a) felsic volcanic rock and in a b) malachite mineral specimen [6]

1.1.2. Emprical Laws

May they be observed as bands (in 1D), circles (in 2D) or shells (in 3D); the spatiotemporal coordination of Liesegang patterns is always very organized and obeys simple empirical laws. For instance, the relative location of the precipitation bands is described by the Jabłczyński law, which defines relative distance of precipitation bands as:

$$1 + p = \frac{x_{n+1}}{x_n}$$

where and x denotes the distance of the rings from the gel – outer solution interface, and n denotes the number of the ring of interest, and 1 + p denotes the so-called "spacing coefficient", which is usually around 1 and very unlikely to be larger than 1.5. Jablczynski's finding was that the ratio of the distances of adjacent rings is a constant and thus they form a geometrical series [7].

An improvement to the above rule is shown "Matalon – Packter Law"[10], which shows that the spacing coefficient that is described in Jablczynski's work, is not a universal quantity but it depends on both on the concentration of the inner electrolyte (doped in the gel) as well as the outer electrolyte (introduced externally). In their work, Matalon and Packter describe the spacing coefficient as;

$$p = f(b_0) + \frac{g(b_0)}{a_0}$$

where p is again the "spacing coefficient", a_0 is the concentration of the outer electrolyte, and b_0 is the concentration of the inner electrolyte. It can easily be seen from the relationship that *p* is a linear function of the outer electrolyte, $1/a_0$, it is also worthwhile to mention that both the intercept, $f(b_0)$, and the slope $g(b_0)$ are decreasing functions [8].

Other than distance between bands, there is also empirical law suggests that band width increases as distance is increased from the gel-outer solution interface by equation:

$$w \propto x_n^{\alpha}, \alpha > 0$$

where w represents width of band, x denotes the distance of the rings from the gel – outer solution interface, n denotes the number of the ring of interest and α is the positive rational number.

Finally, Morse and Pierce found out that time dependency of Liesegang pattern formation can be shown as:

$$x_n = \sqrt{\delta t_n}$$

where t_n is the time elapsed from the beginning to nth band formation and δ is a constant related with the diffusion in the system. x denotes the distance of the rings from the gel – outer solution interface, n denotes the number of the ring of interest. It is not suprising that δ is analogous to diffusion coefficient, because of the fast reaction and slow diffusion [9].

Emprical laws discussed in this section can be applied to most of the Liesegang systems and reaction conditions.

1.1.3. Theoretical Models

There have been discussions about how Liesegang patterns are formed beginning from the discovery of LPs and several theoretical models are suggested to describe the mechanism of LP formation. One of the first theoretical models was developed by Wilhelm Ostwald in 1897 asserted that LPs are the result of repeated cycle of supersaturation, nucleation, and depletion [10]. Local concentration of outer electrolyte in the gel increases as the diffusion proceeds and surpasses a threshold supersaturation concentration. As a consequence, microcrystals start to nucleate and grow, forming discrete precipitation band that finally decreases the ion concentrations in its adjacent zones. Therefore, the precipitate does not form uniformly throughout the gel; rather diffusion of outer electrolyte leads to new supersaturation zone at a farther distance, which results in formation of new precipitation band. Simulations of Liesegang patterns have been done by using this so-called “prenucleation” model and its more complicated variations [10]. Figure 3A illustrates this model.

So-called “postnucleation” model is another theoretical model explains the formation of Liesegang patterns via the competitive formation of tiny crystallites. In this scheme, sol of colloidal particles of sparingly soluble salts uniformly disperse within the gel and Ostwald ripening taking place in the sequel by assembling of tiny colloidal particles which leads to the formation of bigger clusters of precipitation particles. Final step is the self-organization of precipitate into distinct Liesegang patterns that have high amount of crystals and spaces without any crystal. The scheme is described in Figure 3B. Both theories explain Liesegang phemonenon accurately, but still a complete and reliable model that is applicable for all conditions is not developed yet.

A)

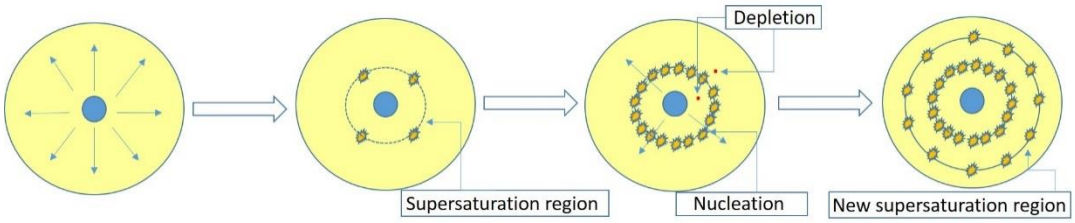

B)

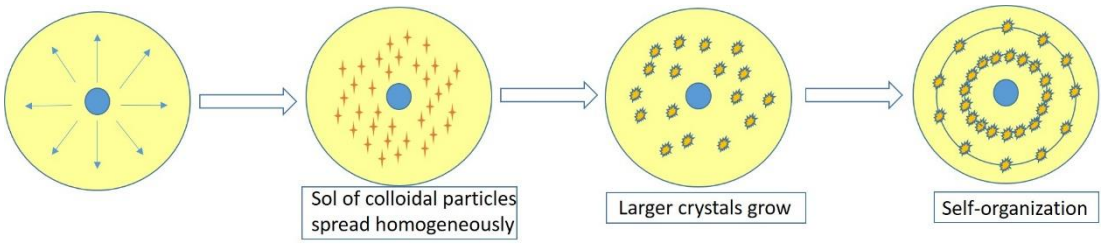

Figure 3. Theoretical models of LP formation. A) The “prenucleation” model, B) The “postnucleation” model

1.1.4. Factors affecting the pattern formation

So far in many studies, the effect of intrinsic and extrinsic factors on the formation of Liesegang patterns were investigated. Matalon and Packter (1955) reported that as outer or inner electrolyte concentration increased, spacing coefficient decreased [8]. Lagzi (2012) reported that as gel concentration increased, spacing coefficient

increased as well [5]. Applying electric field is also another important extrinsic factor that affects LPs, as electric field changes the mass transport of charged chemical substances. Sultan and Halabieh (2000) showed that increase in the potential of applied DC electric field increases spacing coefficient of LPs of $Co(OH)_2$ precipitate [11]. Karam and Sultan (2013) reported the same relation for the AC electric field [12]. Kanazawa and Asakuma (2014) demonstrated that the number of patterns increased with microwave irradiation because polar molecules vibrate and rotate in an electromagnetic field [13]. Furthermore, there are several articles regarding the effect of pH of the gel media on pattern formation [14, 15].

1.1.5. Potential applications

Grzybowski et al. devised a method known as a wet stamping where outer electrolyte is immersed in solid gel stamp and it is placed on gel film containing inner electrolyte [16]. This technique offered a lot of advantages such as eliminating the disturbance of diffusion of co-precipitating ions by hydrodynamic backflow and gave opportunity of formation of Liesegang patterns in micrometer and even nanometer scales. Furthermore, with this method, complex LP geometries could be obtained by changing the shape of stamp (Figure 4). This level of control on synthesis of Liesegang patterns offers an opportunity to design materials that have potential applications in microtechnology and quasi-3D optical elements [16]. Zhao et al. also reported a method by micropatterning of inorganic precipitations in hydrogels with soft lithography that allows design of materials with potential applications in areas such as sensors, colloidal and surface sciences, MEMS, bioengineering and microfluidics [17]. Despite these advances, the fundamental LP research has not led to building of sustainable and feasible applications as mentioned above, presumably because of the limited number of studies in this area.

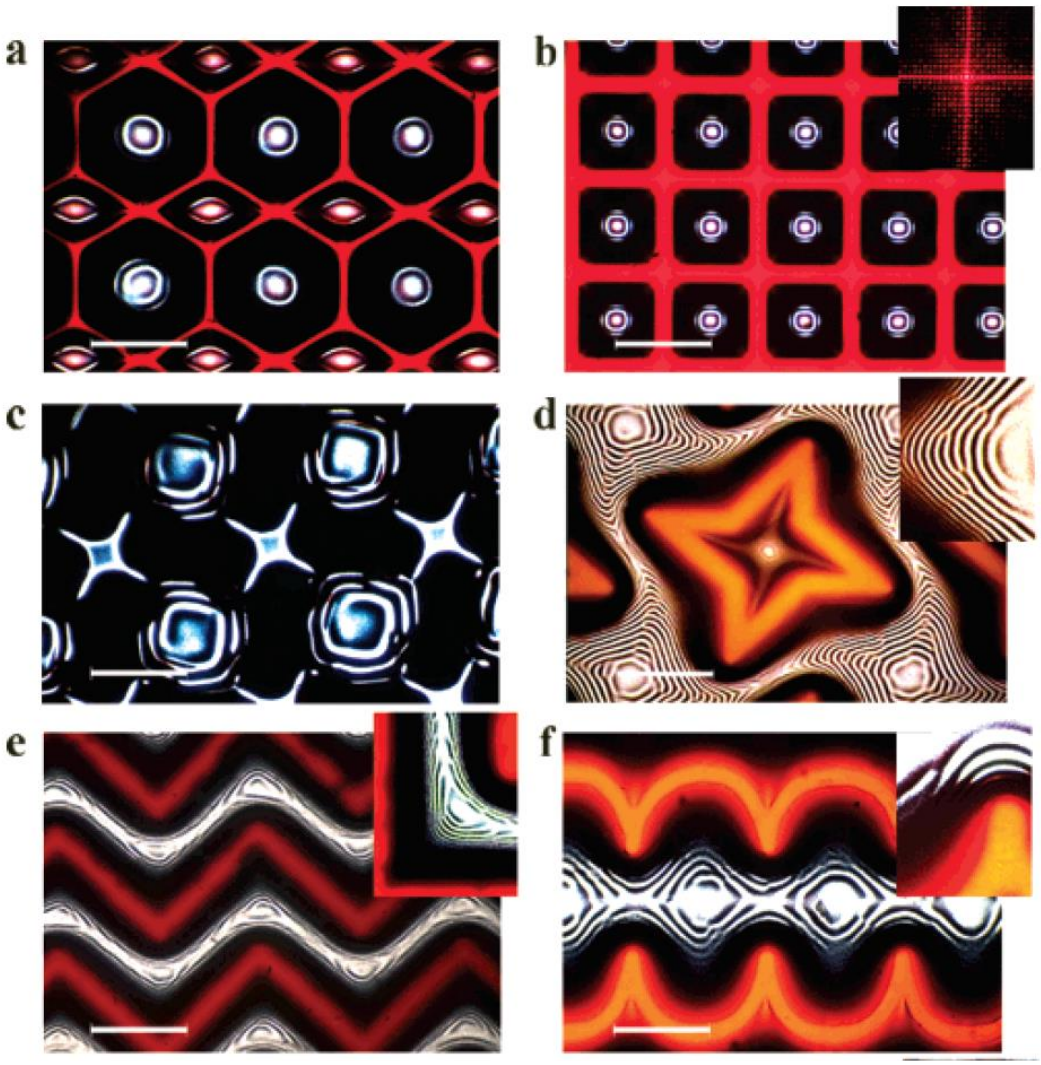

Figure 4. Change of pattern formation with different stamp geometries. (a and b) LP patterns obtained by stamping connected (network) arrays of features corresponding to the red portions of the images. The highly regular array in b was used as a diffraction grating that upon irradiation with a 632-nm laser produced a diffraction pattern shown in the inset. (c) Spiral originating from a stamped pattern of the same chirality. (d) Wedge dislocations propagating along the diagonals of squares between the arms of the stamped stars. (e) Band multiplications develop at the sharp turns in zigzag geometries. Loop-in-band defects around the tips of stamped “spikes” are shown in f. The insets in d-f are close-ups of the dislocations around individual features. [16]

1.2. Stretchable hydrogels and elastic deformation sensors

1.2.1. Hydrogels and polyacrylamide hydrogel

Hydrogels are a unique class of three dimensional cross-linked polymeric networks that can hold a large amount of water inside their network. Over the past century, hydrogels have been effective in material science for a diversity of applications. Hydrophilicity and biocompatibility, combined with soft physical properties close to living systems, make hydrogels valuable in (bio)materials [18] and soft robotics. Especially, stimulus-responsive hydrogels have been very attractive topic due to incredible degrees of control over material properties in response to external stimuli. Up to now, a lot of different stimuli responsive hydrogels are reported including temperature [19], pH [20], chemical [21], light [22], and electro-sensitive [23] hydrogels.

Polyacrylamide hydrogel is a polymer built up with an acrylamide monomer and bisacrylamide crosslinker. Polyacrylamide hydrogels can be made to be highly stretchable. They can be stretched to a high elongations without being torn apart. Polyacrylamide can also be synthesized with different ionic co-monomers as hybrid hydrogels to have supreme mechanical properties, e.g. Sun and Zhao et al. synthesized an extremely stretchable and tough polyacrylamide – alginate hybrid hydrogel (structure is provided in Figure 5) that can be extended up to 21 times of its original length (Figure 6) [24].

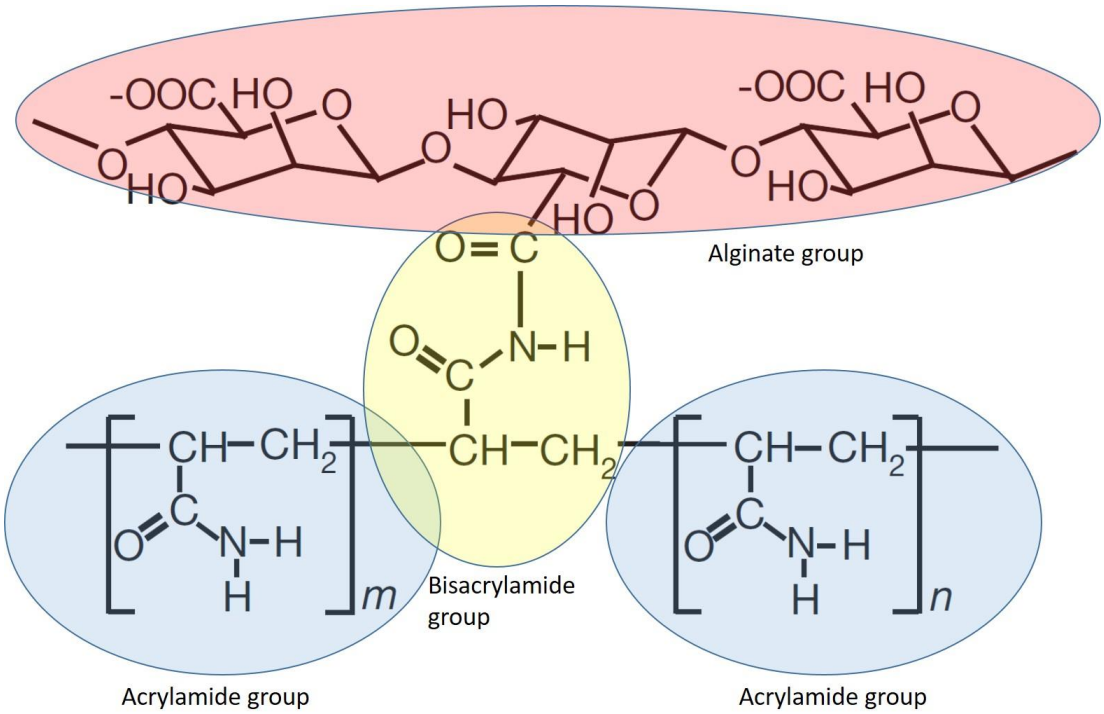

Figure 5. Structure of a polyacrylamide-alginate hybrid hydrogel [24]

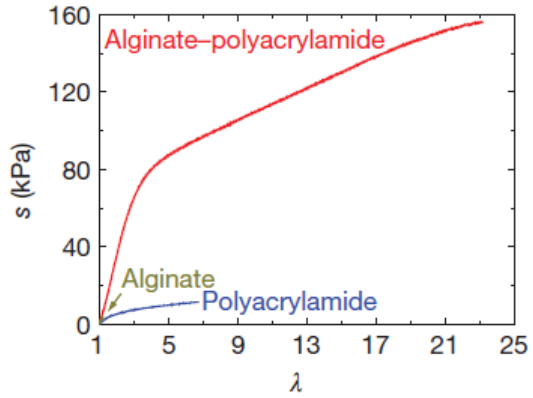

Figure 6. Stress – strain curve of an alginate – polyacrylamide hydrogel in comparison to polyacrylamide hydrogels [24]

1.2.2. Elastic deformation sensor for hydrogels

Macroscopically, plastic deformation of a material is relatively easy to notice and to analyze. However, a material that has been subjected to elastic deformation countless times is macroscopically and analytically very hard, if not impossible, to distinguish from the same material that has not been elastically deformed. Imagine a tennis ball

that has been bounced around, if the ball is not damaged or dirty, would you be able to distinguish it from a brand-new tennis ball?

To assess a material's mechanical properties, mechanical testers are used, which helps to understand how it may respond to stress and when plastic deformation will occur. Mechanical test provides information about the properties such as elasticity, elongation, and tensile strength from the strain – stress curves of a material. While these curves provide experimental data as to the maximum load a material can be subjected to before it starts to plastically deform, it is impossible to probe through mechanical testing, whether a material has gone through some elastic deformation cycles– which is especially important in the case for materials that undergo mostly elastic deformation. Also in real world applications such as in soft robots, it is impossible to make such tests during the operation with the material. Knowing the extend and amount of elastic deformation cycles and their directions can provide crucial information like when to expect the material to start having plastic deformation and where the material is likely to experience a rupture of any kind.

Liu et al. (2017) [25] and Cai et al. (2017) [26] reported wearable stretchable strain sensors by using conductive and elastic hydrogels. Elongation of hydrogel was sensed by monitoring difference in resistance of conductive polyvinyl alcohol hydrogel. Even though sensors manufactured above are reliable and respond fast, there are a lot of electronic parts and needed to be improved to make it easy to operate and make process cheaper. As described in this section, field of elastic deformation sensor for hydrogels is still in its infancy.

1.2.3. The aim of this thesis

In this study, we aim to show that Liesegang patterns can be chemically and mechanically controlled. In section 1.1.4, factors affecting the formation of Liesegang patterns were discussed, it was shown that chemical composition was the one factor that influenced the LP formation the most. In the first part of the project, we aim to show Liesegang formation in novel highly stretchable polyacrylamide - alginate hydrogel and poly-N,N'-dimethylacrylamide hydrogel, and the alteration of patterns

by chemical composition in these gels. These findings, the data in gels other than the so-far reported agarose and gelatin, will help to develop more comprehensive models for Liesegang patterns.

In the second part, we aim to analyze the effect of mechanical stress on Liesegang pattern formation. Mechanical stress, which has not been investigated, yet by any means, may be a key to both promote useful applications of Liesegang patterns and solve the mystery behind them. It can be expected that applying mechanical stress on hydrogels will change the geometry of the gel (i.e. decreasing the thickness of a pseudo 2D gel) and this may increase the diffusion rate and decrease the reaction interface volume, thus Liesegang patterns may change. We aim to develop mechanical deformation sensors involving no electronics by investigating mechanical control of LP patterns. Moreover, the LP patterns in gels that respond chemical and mechanical stimuli can be beneficial in other types of responsive hydrogels research.

CHAPTER 2

2 EXPERIMENTAL

2.1. Materials

For hydrogel preparation, following chemicals are used: acrylamide (AA) (Sigma-Aldrich, 98 % purity), N,N'- dimethylacrylamide (DMAA) (Sigma-Aldrich, 99% purity), N,N'-methylene(bis)acrylamide (BIS) (Sigma-Aldrich, 99% purity), potassium peroxydisulfate (KPS) (Sigma-Aldrich, 99 % purity), sodium alginate (commercial product provided from hammaddeler.com), magnesium nitrate hexahydrate (Merck, 99% purity), sodium hydroxide (Merck, 99% purity), potassium chromate (Merck, 99.5 %), copper (II) chloride dihydrate (Merck, 99 % purity), N,N,N',N'-tetramethylethylenediamine (TEMED) (Sigma-Aldrich, 99% purity), agarose (Fisher bioreagents, for analysis purposes).

For molding agarose stamps, high impact polystyrene (HIPS) is used.

For molding the hydrogels, Plexiglass mold is used.

For mechanical stress setup, Plexiglass and Ecoflex® 00-30 (Smooth-On, Inc.) are used.

2.2. General Experiment Conditions and Setup

2.2.1. Preparation of common materials

2.2.1.1. Preparation of agarose stamp

Wet stamping (WETS) method is used for the formation of the precipitation patterns and Liesegang patterns. A concentrated agarose hydrogel stamp provides the outer electrolyte into a thin hydrogel film containing an inner electrolyte. Preparation of

agarose stamp is as follows: 0.80 g agarose is added to 10 mL DI water. This mixture is heated in microwave for 20 seconds (Be aware that water can evaporate very rapidly and splash, so process should be monitored!). The mixture is heated repeatedly until agarose-water mixture gets homogeneous (generally after 3 cycles of heating for 20 seconds). Homogeneous mixture of agarose and water is poured into cylindrical high impact polystyrene (HIPS) mold (that is printed by aid of Zortrax 3D printer) with diameter of 10 mm and height of 8 mm. Molded mixture is put to refrigerator for 15 minutes. Finally, after it gets solid, we put them to outer electrolyte solution for 30 minutes which is the time needed for all water inside the agarose stamp exchanges with outer electrolyte solution.

2.2.1.2. Preparation of Ecoflex substrate

Ecoflex substrate is used as a substrate for polyacrylamide hydrogel to achieve better stretching since Ecoflex is a better elastomer than polyacrylamide hydrogel and its' shape will not change after elastic deformation. Preparation of Ecoflex substrate is as follows: 12.5 g Ecoflex A (Smooth-On, Inc.) and 12.5 g Ecoflex B (Smooth-On, Inc.) are mixed together and poured to a plexiglass mold with dimensions 10 cm*14 cm*2 mm. 2 commercial tea stirring wooden sticks are placed on uncured Ecoflex with a 7 cm distance apart from each other (which is width of the hydrogel). The reason of putting these wooden sticks is that polyAA hydrogel easily slips on Ecoflex and there is a little adhesion. So, wooden sticks help to avoid slippage of polyAA gel on Ecoflex substate since hydrogel will adhere to wood better than Ecoflex (Figure 9). So, Ecoflex blends with the wooden sticks during the curing process. Then, uncured ecoflex-wood compoiste is put to oven at 60 $^{\circ}$C and kept for 45 minutes in it. Finally, Ecoflex-wood composite is taken out from the oven and allowed to cool down.

2.2.2. Preparation of hydrogels

2.2.2.1. Preparation of polyacrylamide – alginate hybrid hydrogel

For the synthesis of thin polyacrylamide gel, 1.244 g AA and 0.001 g crosslinker BIS are added to 8.6 g DI water. This mixture is subjected to nitrogen gas for 30 minutes to get rid of oxygen gas dissolved in water which reacts with photo-initiator KPS during the polymerization process. Then, 0.03 g of photo-initiator KPS and 0.0308 g

$Mg(NO_3)_2.6H_2O$ are added. 10 microliter of crosslinking accelerator TEMED is added. Finally, 0.156 g sodium alginate is added to petri dish and then prepared solution poured to petri dish. Alginate is dissolved in solution. Then, petri dish is covered with the another plastic matter (lid of petri dish) to compress the solution.

2.2.2.2. Preparation of poly-DMAA hydrogel

For the preparation PDMMA hydrogel, 1.6 mL DMMA is added to 6.4 mL DI water and stirred. This mixture is subjected to nitrogen gas for 30 minutes to get rid of oxygen gas dissolved in water which reacts with photo-initiator KPS during the polymerization process. 0.07 g KPS and 0.25 g $Mg(NO_3)_2 \cdot 6\ H_2O$ are added to prepared solution. Finally, 5 microlitre TEMED is added and pre-gel solution is poured to petri dish. Pregel solution in petri dish is compressed with a lid of petri dish to get smooth surface. Gelation is completed after 24 hours.

2.2.2.3. Preparation of polyacrylamide hydrogel

1.446 g acrylamide and 0.006 g bis-acrylamide are dissolved in 9.2 mL water. The solution is degassed for 20 minutes by keeping the solution in the vacuum. 0.02 g potassium peroxydisulfate and 0.02 g potassium chromate (0.01 M) are added to the degassed solution, followed by the addition of 10 µL TEMED. After 10 minutes, this final solution is poured to the Plexiglass mold with 7 cm x 7 cm x 2 mm dimensions (Figure 8). Molded pre-gel solution is left at 20 ˚C and 0.9 atm, for 24 hours for gelation process.

2.2.3. Pattern formation and setup for stretching experiments

2.2.3.1. Pattern formation and mechanical stress setup for polyAA-alginate hybrid hydrogels

After 1 day, when gelation process is completed, %8 agarose stamp is put in 2 M NaOH solution and after 30 minutes, this stamp is placed on the center of the gel. Then, petri dish containing the gel is firmly closed and the lid is wrapped with parafilm. 24 hours is given for the formation precipitation patterns (PP) in gel. Experiments are conducted at 20 ˚C and 0.9 atm. The temperature is a significant

factor that affects the PP formation and care has to be taken not to change temperature during the formation of the PP patterns!

For applying mechanical stress, hydrogel is cut into a rectangular shape with dimensions of 7 cm x 5 cm x 2 mm. One of the shorter side of the gel is covered with lamels and clamped. The other side is also covered with lamels and is stretched manually. After reaching to desired extent of stretching (vide supra), other side is fixed by using two strong magnets. The setup described is illustrated in Figure 7.

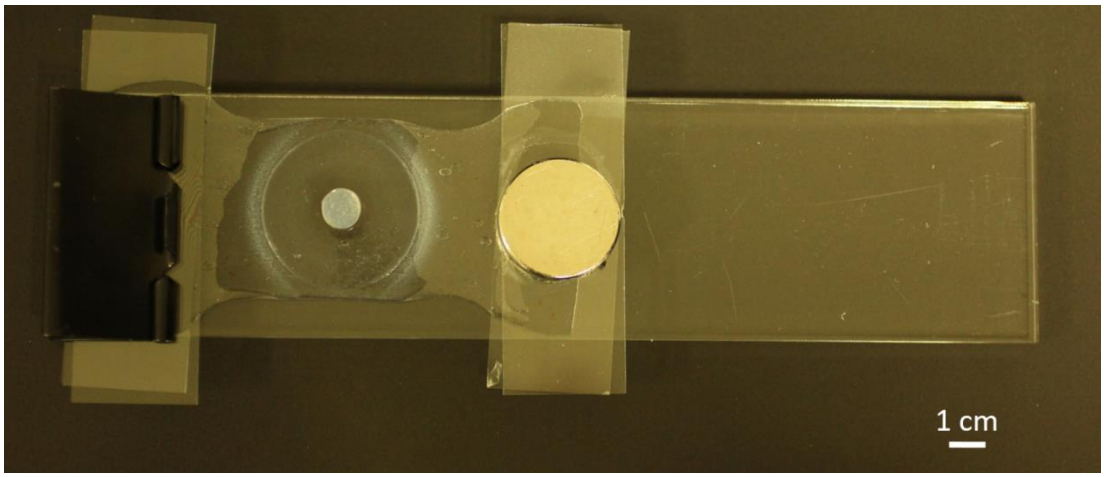

Figure 7. The setup of our 'stretching experiments' for polyAA-alginate hybrid hydrogels.

2.2.3.2. Pattern formation for poly-DMAA hydrogels

Then, agarose stamp saturated with outer electrolyte (3 M NaOH) is placed to the surface of the hydrogel at its center. Precipitation pattern formation is completed 24 hours after stamp is placed. Patterns are analyzed for the distances at which the rings start to from the edge of the agarose stamp. Experiments are conducted at 20 ˚C and 0.9 atm. The temperature is a significant factor that affects the PP formation and care has to be taken not to change temperature during the formation of the PP patterns!

2.2.3.3. Pattern formation and mechanical stress setup for poly-AA hydrogels

Prepared polyacrylamide hydrogel is transferred to Ecoflex® 00-30 substrate with dimensions 14 cm x 10 cm x 2 mm, which has embedded wooden sticks in it for better

adhesion of the gel to the substrate (Figure 9). A set of 6 samples with different elongations are prepared: unstretched, 10 %, 20 %, 30 %, 40 % and 50 % stretched. Stretching setup is shown in Figure 10. An agarose stamp supplies the outer electrolyte (1 M $CuCl_2 \cdot 2H_2O$) into the thin polyacrylamide film containing a co-precipitating inner electrolyte (0.01 M K_2CrO_4). Stamps are placed in the center of each sample's surface as shown in Figure 11. Outer electrolyte diffuses into the gel after stamp is placed and Liesegang patterns start to form around the stamp. Samples are placed in closed plastic containers, which have sprayed water to minimize water evaporation in hydrogels and left for 24 hours for pattern formation. Photos of samples are taken after 24 hours. Then, samples are released from mechanical stress and photos are taken again. Finally, in 18 hours after releasing the stress (42 hours after placing the stamp), photos are taken for the last time. Figure 12 summarizes the whole process.

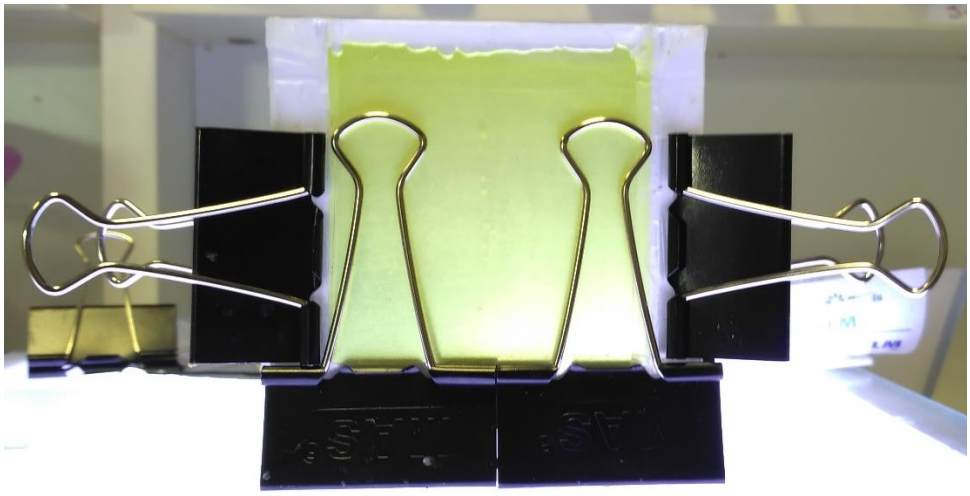

Figure 8. Mold used for gelation of polyacrylamide gel

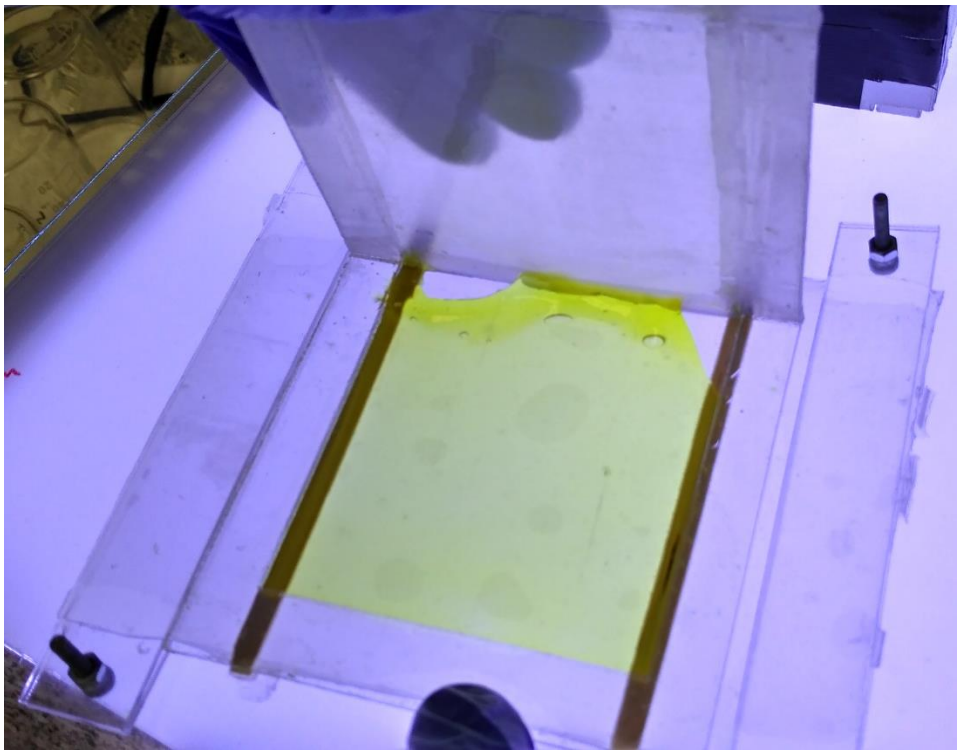

Figure 9. Ecoflex substrate with wooden sticks embedded in it

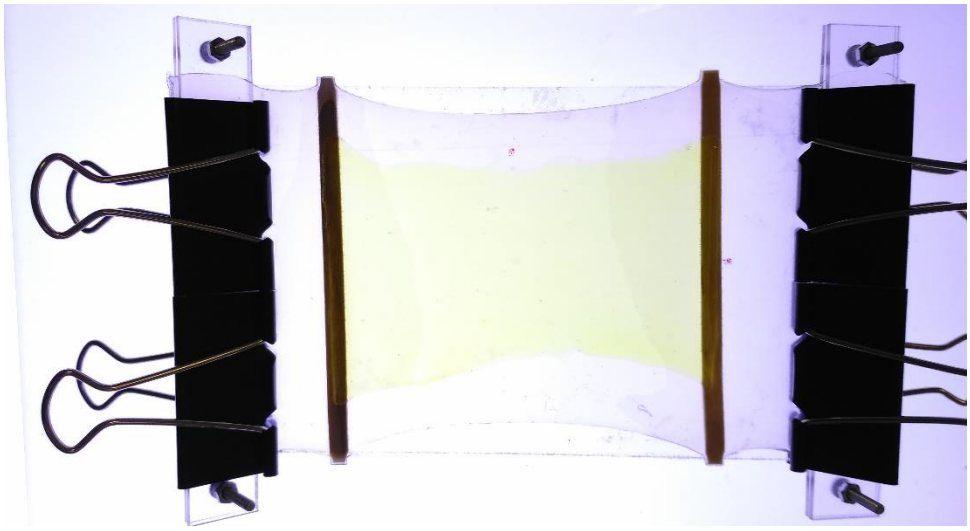

Figure 10. Mechanical stress setup for polyacrylamide hydrogel. Polyacrylamide hydrogel is placed on Ecoflex, which is placed on Plexiglass substrate and stretched. Clamps are used for fixing the Ecoflex substrate.

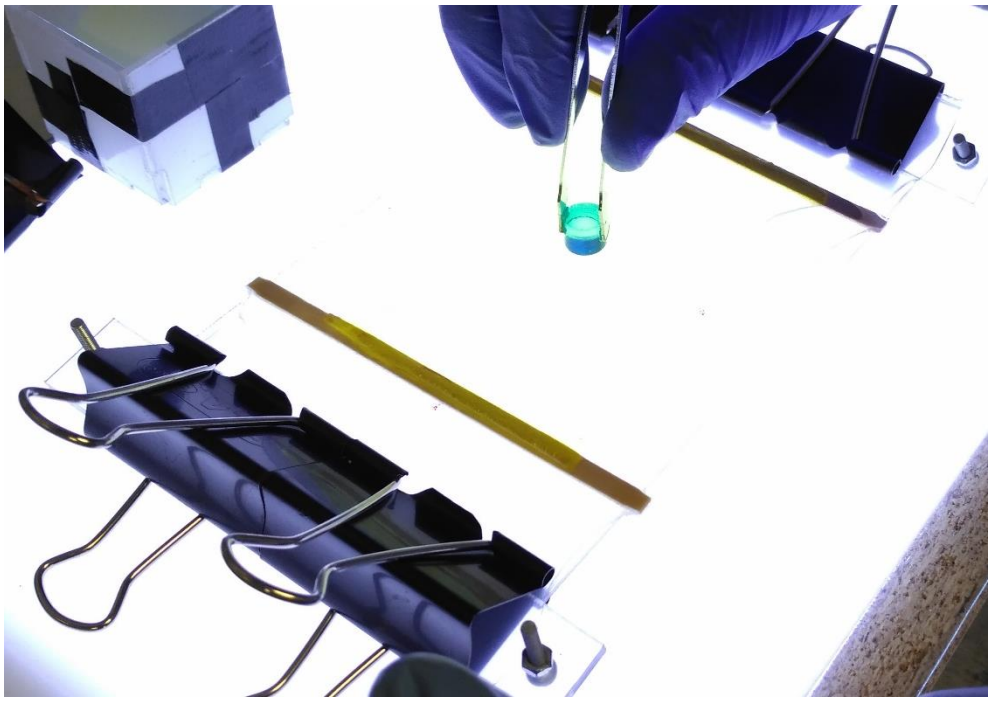

Figure 11. Placing of stamps with outer electrolyte into the center of the polyacrylamide gel.

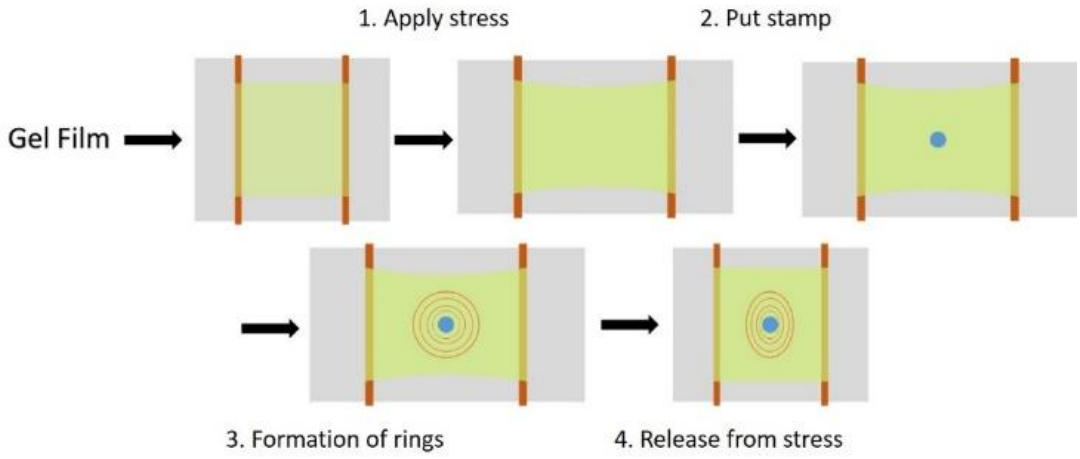

Figure 12. Liesegang pattern formation in hydrogel and mechanical stress setup

2.3. Instrumentation

2.3.1. Camera

Photos of the samples are captured with Canon EOS REBEL T2i DSLR camera (dimensions are 5184 x 3426 pixels, focal length is 50 mm, resolution is 72 dpi). Images are analyzed by using public-domain software ImageJ. For Section 3.1, distances of patterns are calculated from the outer edge of the stamp (reference point), whereas for Section 3.2, distances of patterns are calculated from the center of the stamp (reference point). For Section 3.1, starting distance means the distance where precipitation starts and finishing distance means the distance where precipitation finishes.

CHAPTER 3

3 RESULTS & DISCUSSIONS

3.1. Chemical and mechanical control of simple precipitation patterns

As an initial chemical system for preparation of Liesegang patterns, we have selected a common and simple precipitation reaction, which only forms one ring in the pseudo 2D gels we prepare, rather than the more complex, multi-ring Liesegang pattern. The precipitation reaction we selected was:

$$Mg^{2+}(aq) + 2\,OH^{-}(aq) \rightarrow\ Mg(OH)_2(s)$$

This reaction proceeds and forms the mentioned precipitation ring of magnesium hydroxide, as the inner electrolyte (magnesium ion) is subjected to the outer electrolyte (hydroxide) that is diffused into the gel through the application stamp (for experimental details on preparation of the stamp and gels, see section 2.2). The formed precipitation ring has distinct starting and finishing distances from the stamp. We analyzed the precipitation rings forming under different experimental conditions (see below) according to their starting and finishing distances (for details about measurements of distances, see section 2.3).

3.1.1. Effect of inner electrolyte concentration change in PAA-Alg hydrogels

As noted in section 1.1.4., concentrations of chemicals determine the shapes of precipitation patterns. Change of precipitation patterns as a function of change in an inner electrolyte (magnesium ion) concentration is given in Figure 13. Calculated

precipitation pattern distances as a function inner electrolyte concentration is given in Figure 14. It is obvious from Figure 14, as concentration of inner electrolyte increases, rings start to form and finish at a closer distance from the stamp. This can be explained by the fact that as inner electrolyte concentration increases in the gel, supersaturation threshold will be reached relatively in less time and precipitate tends to form sooner. This indicates precipitation pattern will form at a closer distance as inner electrolyte concentration increases.

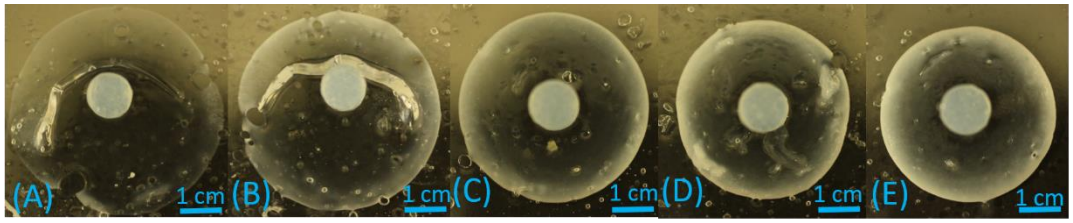

Figure 13. Change of precipitation patterns due to change of inner electrolyte concentration at constant outer electrolyte (hydroxide ion) concentration 1 M and at inner electrolyte (magnesium ion) concentrations : (A) = 0.014 M, (B) = 0.028 M, (C) = 0.042 M, (D) = 0.056 M, (E) = 0.070 M; acrylamide = 12.22 %; alginate = 1.53 %; BIS = 0.01 %; TEMED = 0.085 %; KPS = 0.25 %; (T= 20 ˚C).

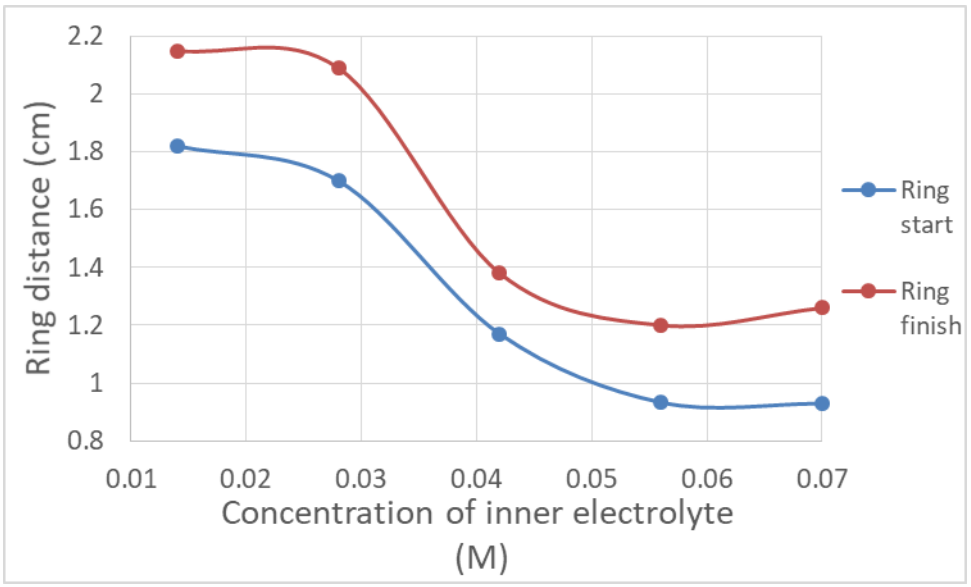

Figure 14. Calculated precipitation pattern distances as a function of inner electrolyte concentration.

3.1.2. Effect of outer electrolyte concentration change in PAA-Alg hydrogels

Change of precipitation patterns as a function of an outer electrolyte (hydroxide ion) concentration is given in Figure 15. Calculated precipitation pattern distances as a function inner electrolyte concentration is given in Figure 16. As concentration of outer electrolyte increases, rings start and finish to form from the farther distance from the stamp. Possible explanation to this trend can be the fact that as outer electrolyte concentration increases, inner electrolyte concentration will decrease more at areas adjacent to the stamp. As a consequence, this will create greater inner electrolyte concentration flux from gel to the areas adjacent to stamp and inner electrolyte in the gel decrease. So, supersaturation threshold will reach at farther distance and allowing the formation of precipitation pattern at farther distance.

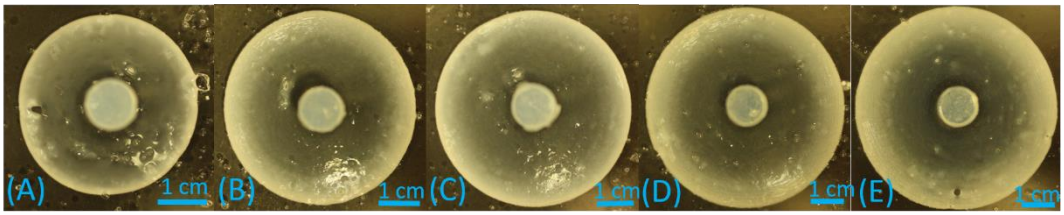

Figure 15. Change of precipitation patterns due to change of outer electrolyte concentration at constant inner electrolyte (magnesium ion) concentration 0.07 M and at outer electrolyte (hydroxide ion) concentrations : (A) = 2 M, (B) = 3 M, (C) = 4 M, (D) = 5 M, (E) = 6 M; acrylamide = 12.22 %; alginate = 1.53 %; BIS = 0.01 %; TEMED = 0.085 %; KPS = 0.25 %; (T= 20 $^{\circ}$C).

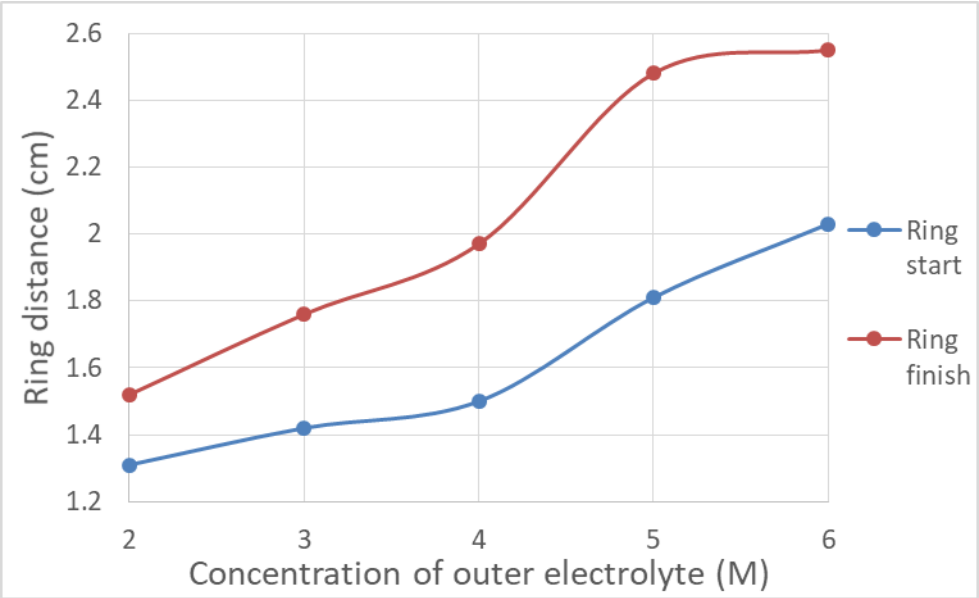

Figure 16. Calculated precipitation pattern distances as a function of outer electrolyte concentration.

3.1.3. Effect of acrylamide concentration change in PAA-Alg hydrogels

Change of precipitation patterns as a function of acrylamide concentration is given in Figure 17. Calculated precipitation pattern distances as a function acrylamide concentration is given in Figure 18. Ring distances reach the top point at 6.77% by mass. Other than that, acrylamide concentration seems to have no significant effect on distances of rings.

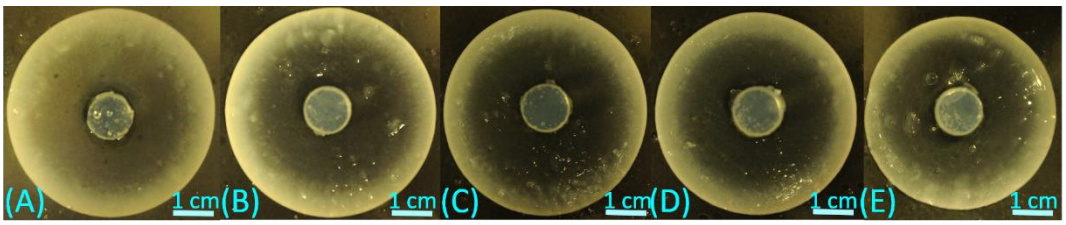

Figure 17. Change of precipitation patterns due to change of acrylamide concentration at constant inner electrolyte (magnesium ion) concentration 0.07 M and at constant outer electrolyte (hydroxide ion) concentration 2 M and at acrylamide concentrations: (A) = 5.49 % , (B) = 6.77 %, (C) = 8.01 %, (D) = 9.23 %, (E) = 10.41 %; alginate = 1.04%; BIS = 0.01 %; TEMED = 0.1 %; KPS = 0.25 %; (T= 21 $^{\circ}$C).

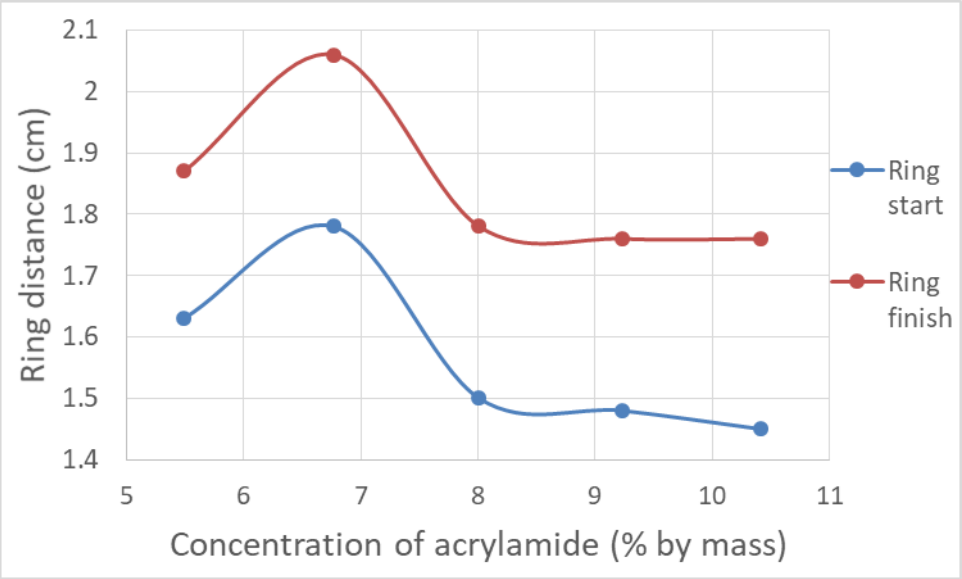

Figure 18. Calculated precipitation pattern distances as a function of acrylamide concentration.

3.1.4. Effect of alginate concentration change in PAA-Alg hydrogels

Change of precipitation patterns as a function of change in an alginate concentration is given in Figure 19. Calculated precipitation pattern distances as a function alginate concentration is given in Figure 20. Distances, at which ring start do not depend on alginate concentration significantly. On the other hand, distance where ring finishes depend on alginate concentration. The distance where the rings finish increases as concentration of alginate increases with the exception of 0.26 % alginate concentration, which has a same distance as that observed with alginate concentration of 1.27 %. Increasing of the finishing distance can be explained with increasing of impurities (alginate in this case) in the gel [5]. When the amount of impurities increase in the gel, it will give small precipitation crystals more site and area to nucleate and grow into bigger crystals. So, as alginate amount increases, nucleation will continue to form at farther distances and precipitation bands will finish at farther points.

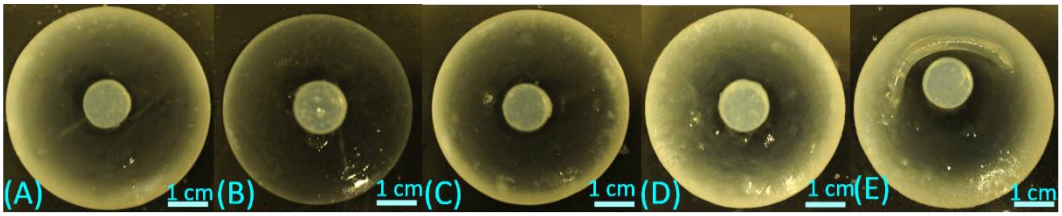

Figure 19. Change of precipitation patterns due to change of alginate concentrations at constant inner electrolyte (magnesium ion) concentration 0.07 M and at constant outer electrolyte (hydroxide ion) concentration 2 M and at alginate concentrations: (A) = 0.26 % , (B) = 0.51 %, (C) = 0.77 %, (D) = 1.02 %, (E) = 1.27 %; acrylamide = 12.25 %; BIS = 0.01 %; TEMED = 0.1 %; KPS = 0.25 %; (T= 20 ˚C).

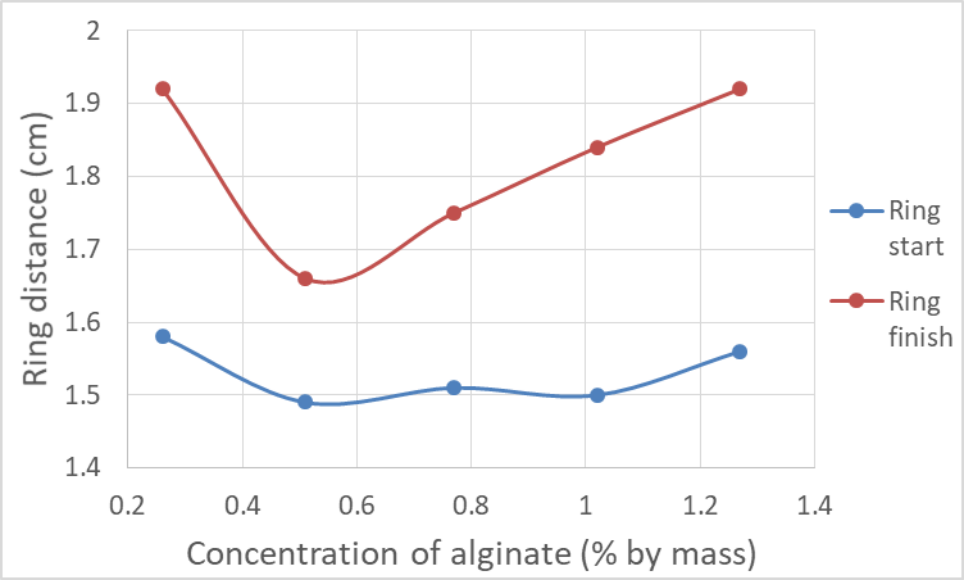

Figure 20. Calculated precipitation pattern distances as a function of alginate concentration.

3.1.5. Effect of inner electrolyte and DMMA concentration change in PDMMA gels

We also worked on a chemically different gel medium, poly-N,N'–dimethylacrylamide hydrogel (DMMA) for formation of the precipitation patterns, to see how this affects

the formation of the precipitation patterns. In Figure 21, the precipitation patterns in hydrogels with different DMMA concentration are shown. As DMMA concentration increased, precipitation patterns start to form at farther distances from the stamp (Figure 22).

In Figure 23, precipitation patterns in hydrogels with different inner electrolyte concentration and at constant DMMA concentration (20% DMMA by mass) is shown. As inner electrolyte concentration increased, precipitation patterns start to form at closest fronts from the stamp (Figure 24). It is the same trend observed in PAA – alginate hybrid gel.

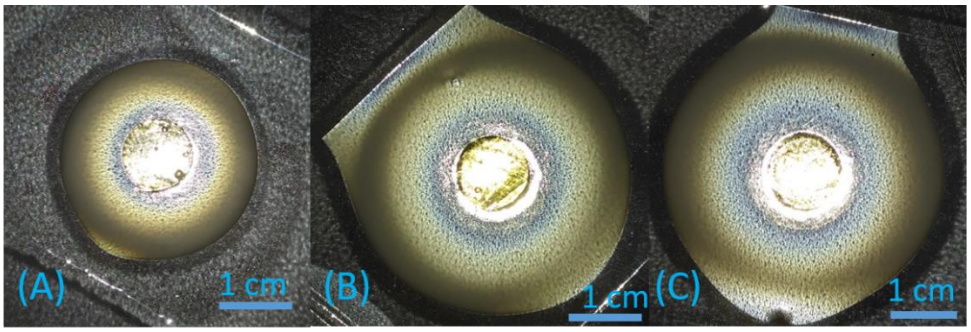

Figure 21. Precipitation patterns in DMMA gels with DMMA concentrations by mass: A) 15 %, B) 20% and C) 25 %. Concentration of inner electrolyte (Magnesium ion) is 0.157 M and outer electrolyte (hydroxide ion) is 6 M. Concentrations of KPS is 0.85 % by mass and TEMED is 0.0001 % by mass. (T= 26 ˚C).

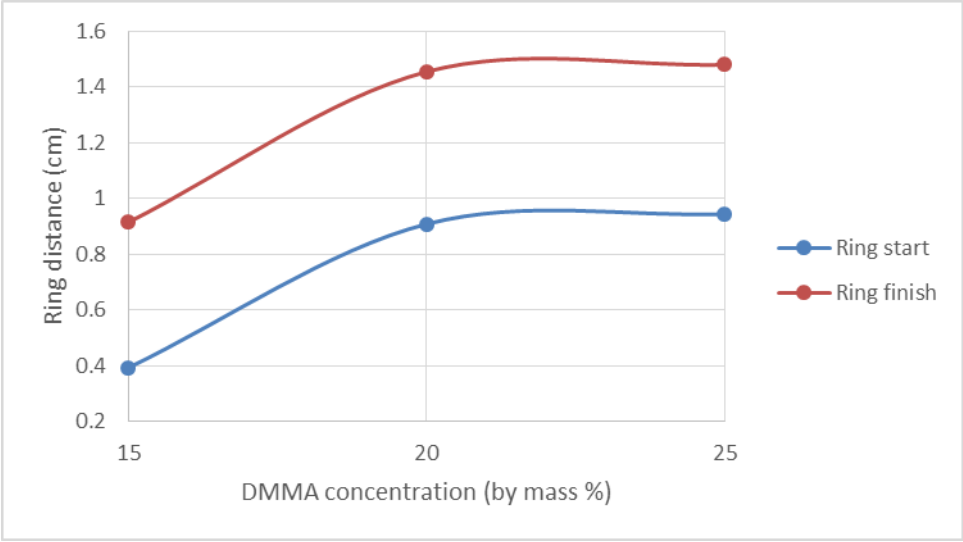

Figure 22. Calculated precipitation pattern distances as a function of DMMA concentration.

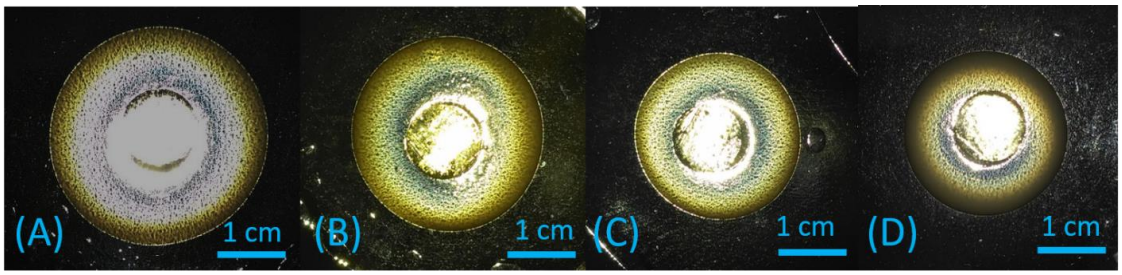

Figure 23. Precipitation patterns in DMMA gels at inner concentration (magnesium ion concentration) of: (A) 0.146 M, (B) 0.171 M, (C) 0.195 M, and (D) 0.220 M. Outer electrolyte concentration (hydroxide ion) is 3 M. Concentration of gel is 20 % by mass of DMAA. Concentrations of KPS is 0.85 % by mass and TEMED is 0.0001 % by mass. (T= 21 ˚C).

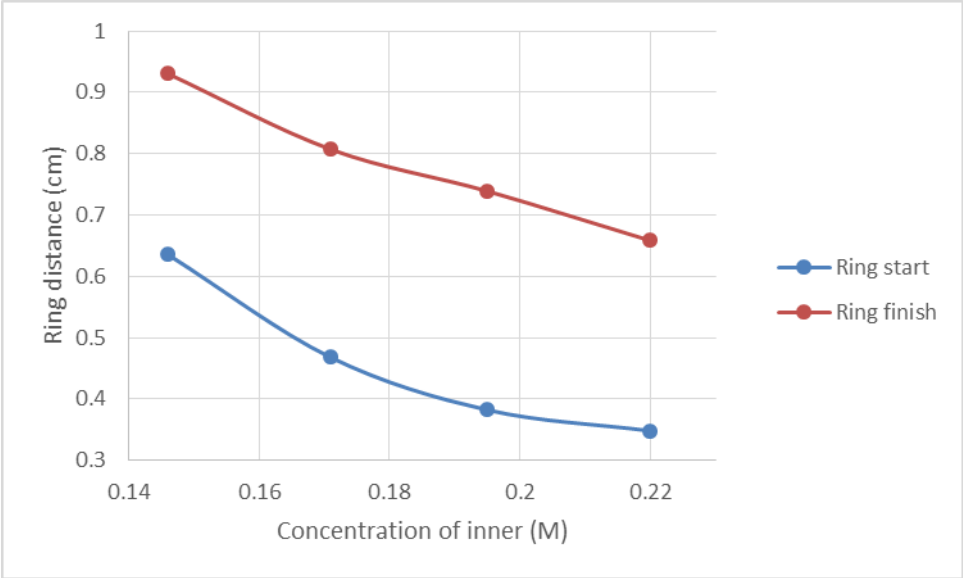

Figure 24. Calculated precipitation pattern distances as a function of inner electrolyte concentration.

3.1.6. Mechanical stress experiment

After assessing the effect of other parameters of the gel formation, we selected one gel system to investigate the effect of mechanical input on the pattern formation. Gels with the same composition were stretched at different percent elongations to see the effect of magnitude of elongation on precipitation patterns. This is illustrated in Figure 25. It is observed that as mechanical stress is increased on gel, the

precipitation patterns became more oval, after the release of mechanical input. Graph given in Figure 26 shows the obtained ovalities at different percent elongations.

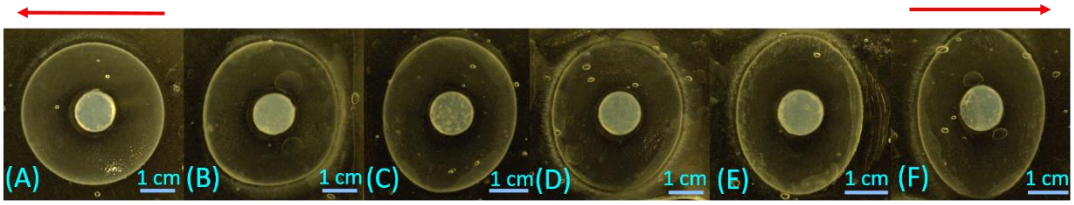

Figure 25. Mechanical stress tests for different percentage elongations for gels that have same composition. Arrows show the direction of applied mechanical stress. (A) Unstretched reference gel, (B) 10% stretched after release of mechanical stress, (C) 20% stretched after release of mechanical stress, (D) 30% stretched after release of mechanical stress, (E) 40% stretched after release of mechanical stress, and (F) 50% stretched after release of mechanical stress. Concentration of inner electrolyte (Magnesium ion) is 0.07 M and outer electrolyte (hydroxide ion) is 3 M. Concentrations of KPS is 0.17 % by mass, alginate is 1 %, BIS is 0.01 % and TEMED is 0.00005 % by mass. T = 26 $^{\circ}$C.

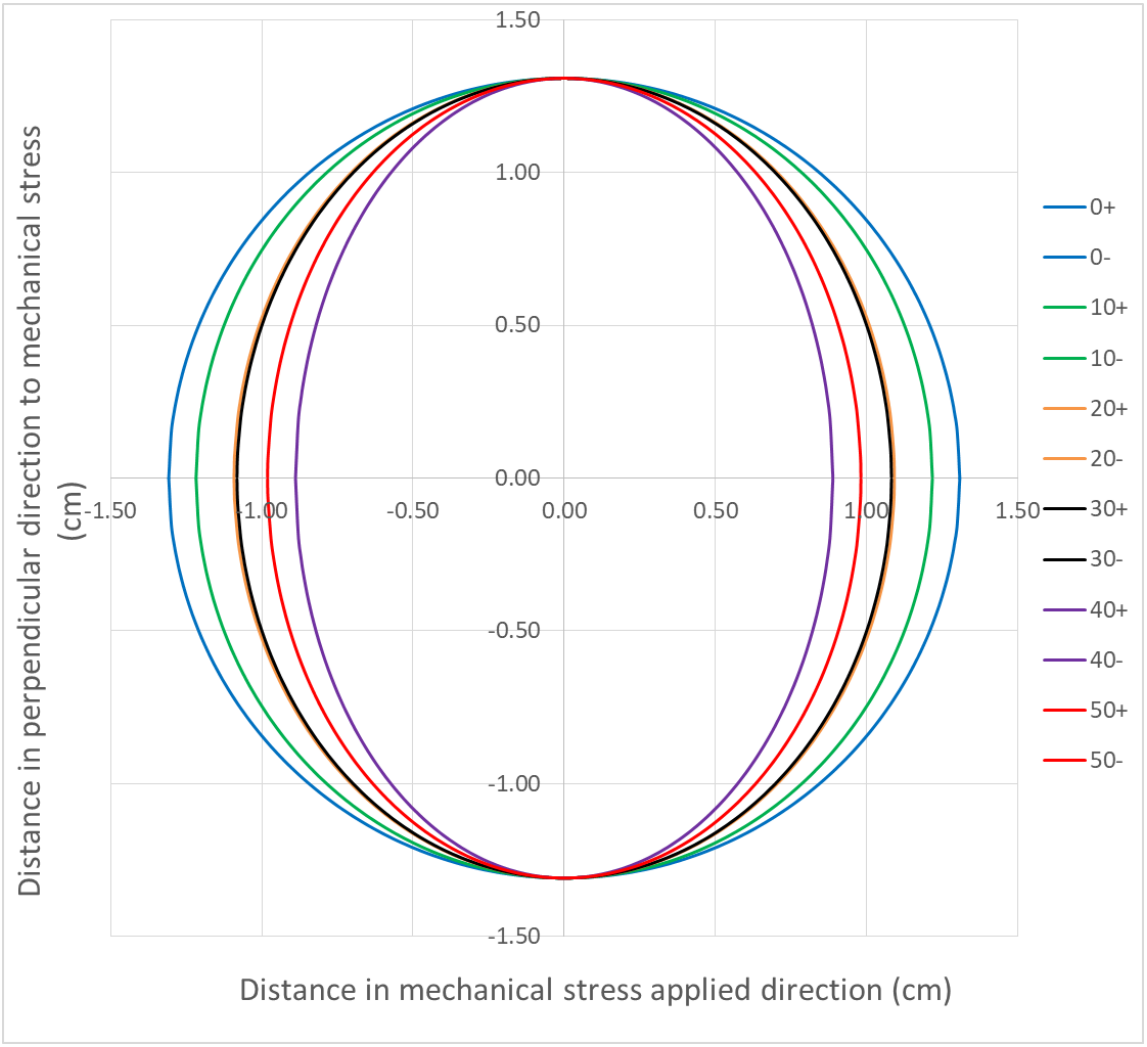

Figure 26. Precipitation patterns shapes at different percent elongations. The distances in the direction perpendicular to the applied stress is normalized to the same value to display the deviations from perfect circle (unstretched).

3.2. Mechanical control of Liesegang patterns

After investigating the effect of chemical composition and mechanical stress on simple precipitation patterns, we focused on more detailed investigation of the effect of mechanical stress on reaction-diffusion systems. For this purpose, applying mechanical stress on Liesegang patterns was our next step, since it will give more information about effect of mechanical stress due to formation of multiple of bands with distinct spacing coefficient, and in particular, spread over a time interval. The

hydrogel used for LP formation was polyacrylamide hydrogel (without alginate). The precipitation reaction we selected was:

$$Cu^{2+}(aq) + CrO_4^{2-}(aq) \rightarrow CuCrO_4(s)$$

LP formation was monitored and analyzed according to following 3 steps: 1) pattern formation while hydrogel is stretched (24 hours after stretching), 2) immediate release of mechanical stress on hydrogel after 24 hours of stretching and 3) pattern formation after release of mechanical stress (18 hours after releasing the hydrogel and 42 hours in total from the beginning of experiment).

3.2.1. Liesegang patterns formed while stress is applied

We prepared the stamp and gel and placed them in the stretching setup as described earlier in the Experimental part. Pattern formation was monitored for the following percentage elongations for hydrogels that have same chemical composition (inner electrolyte (chromate ion) = 0.01 M, outer electrolyte (copper (II) ion) = 1 M, acrylamide = 13.5 w%, BIS = 0.056 w%, KPS = 0.187 w%, TEMED = 0.0001 w%) : 0 %, 10 %, 20 %, 30 %, 40 %, and 50 %. Each stretching experiment was repeated with four identical samples at different runs. In Figure 27, Liesegang patterns formed after 24 hours of stretching are illustrated. For investigation of change in the reaction-diffusion in different elongations, radii of the last rings formed are calculated. In Figure 28, these radii obtained for each elongation are illustrated. It shows that there is no significant change in reaction-diffusion since radii of the last rings are similar to each other. It can be explained as following: hydrogels are mostly consists of high amount of water (87 % by weight in our hydrogel) and any (mild) elastic deformation will not change the total volume of the hydrogel; it will only decrease the thickness of the hydrogel. Thus, concentration of the inner electrolyte in hydrogel will not change. Since the diffusion is dependent on concentration gradient and precipitation reaction is dependent on concentration, reaction-diffusion system is not altered by the applied mechanical stress. Moreover, the distances between bands for different elongations are provided in Figure 29. These distances between bands increase as

the band number increase in geometric series as expected. Data can be fit to linear equation since spacing coefficient is too close to 1 (R^2 values are close to 1 as shown in Figure 29). Slopes obtained from the linear fit of data obtained at different elongations are close to each other, which mean spacing coefficients of all rings are similar in the samples subjected to different elongations. This data also provides a proof of no change in reaction-diffusion mechanism by applying mechanical stress.

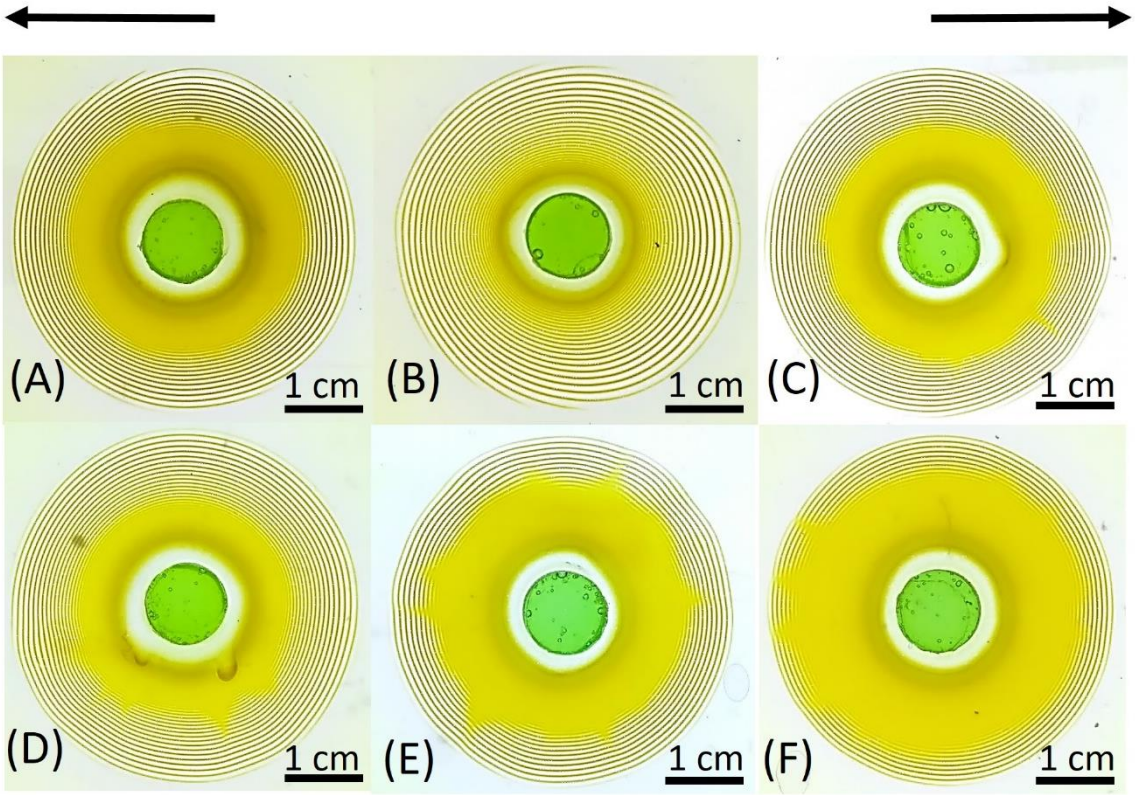

Figure 27. Liesegang patterns in stretched samples after 24 hours of stretching. A) 0 % percentage elongation, B) 10 % percentage elongation, C) 20 % percentage elongation, D) 30 % percentage elongation, E) 40 % percentage elongation, F) 50 % percentage elongation. Arrows show the direction of applied mechanical stress. Concentrations of components are as follows: inner electrolyte (chromate ion) = 0.01 M, outer electrolyte (copper (II) ion) = 1 M, acrylamide = 13.5 w%, BIS = 0.056 w%, KPS = 0.187 w%, TEMED = 0.0001 w%. T = 20 °C.

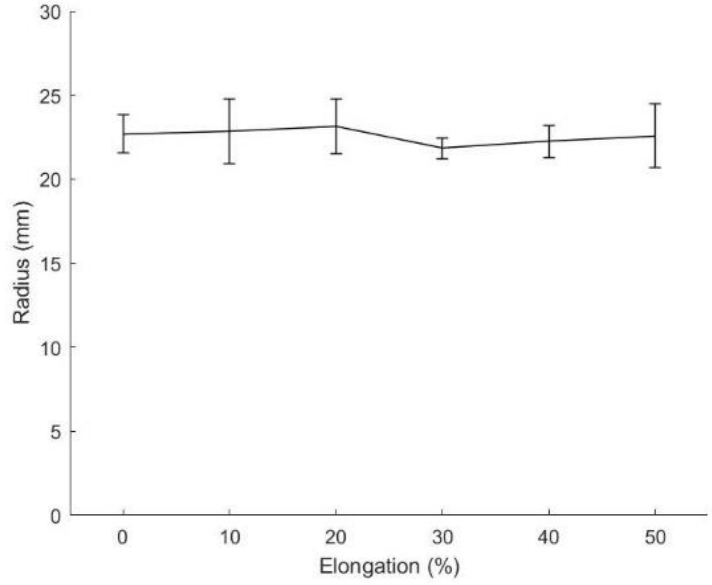

Figure 28. Radii of final rings in stretched samples vs. percentage elongation.

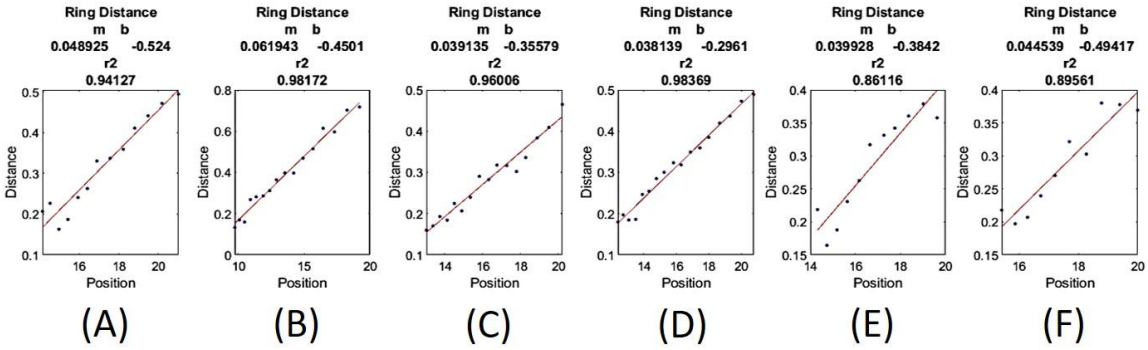

Figure 29. Position of the rings vs. distance between the bands. Position (x_n) is the distance from gel-stamp interface in mm and distance between the bands is also in mm scale. Dots in the graph consecutive ring bands as band number (n) increases to the right. This graph shows that as band number increases, distance between the bands increase as well since bands increase in geometric series. Data can be fit to linear equation since spacing coefficient is too close to 1 (in graph m is the slope and b is y-intercept). R^2 values are close to 1 which means it fits linear equation well.

3.2.2. Liesegang patterns immediately after release of stress

Mechanical stress applied to hydrogel was released after 24 hours. There was no change in dimensions of the hydrogel compared to before applying mechanical stress and it shows that deformation was totally elastic. Figure 30 shows how circular ring patterns turn into more oval shapes as elongation increases. Radii of the last rings decrease in direction of applied mechanical stress and increase in the direction perpendicular to mechanical stress. For better illustration, Figure 31 provides a Cartesian coordinate of the last ring radiuses at different elongations. Moreover, aspect ratios of elliptical shapes are calculated and shown in Figure 32. The aspect ratio of a shape describes the proportional relationship between its height and its width ($aspect\ ratio = {}^{height}/_{width}$). Aspect ratio increases as elongation increases. Data can be fit to a line and has R^2 value of 0.995. We discussed that applying mechanical stress to hydrogel medium does not alter reaction-diffusion system in section 3.2.1. So, the change in shapes of patterns is solely due to the geometry change, when the samples are stretched.

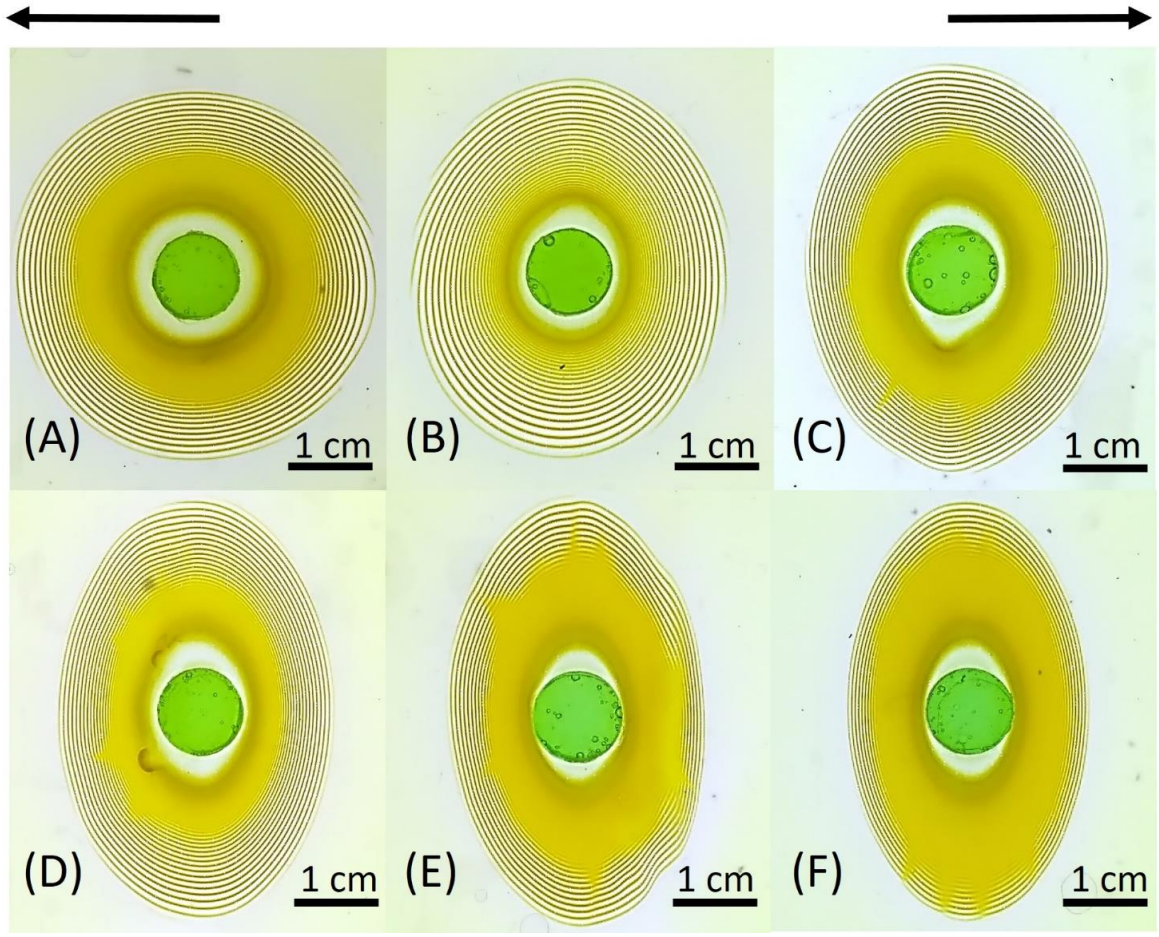

Figure 30. Liesegang patterns immediately after release of mechanical stress. A) 0 % percentage elongation, B) 10 % percentage elongation, C) 20 % percentage elongation, D) 30 % percentage elongation, E) 40 % percentage elongation, F) 50 % percentage elongation. Arrows show the direction of applied mechanical stress. Concentrations of components are as follows: inner electrolyte (chromate ion) = 0.01 M, outer electrolyte (copper (II) ion) = 1 M, acrylamide = 13.5 w%, BIS = 0.056 w%, KPS = 0.187 w%, TEMED = 0.0001 w%. T= 20 °C.

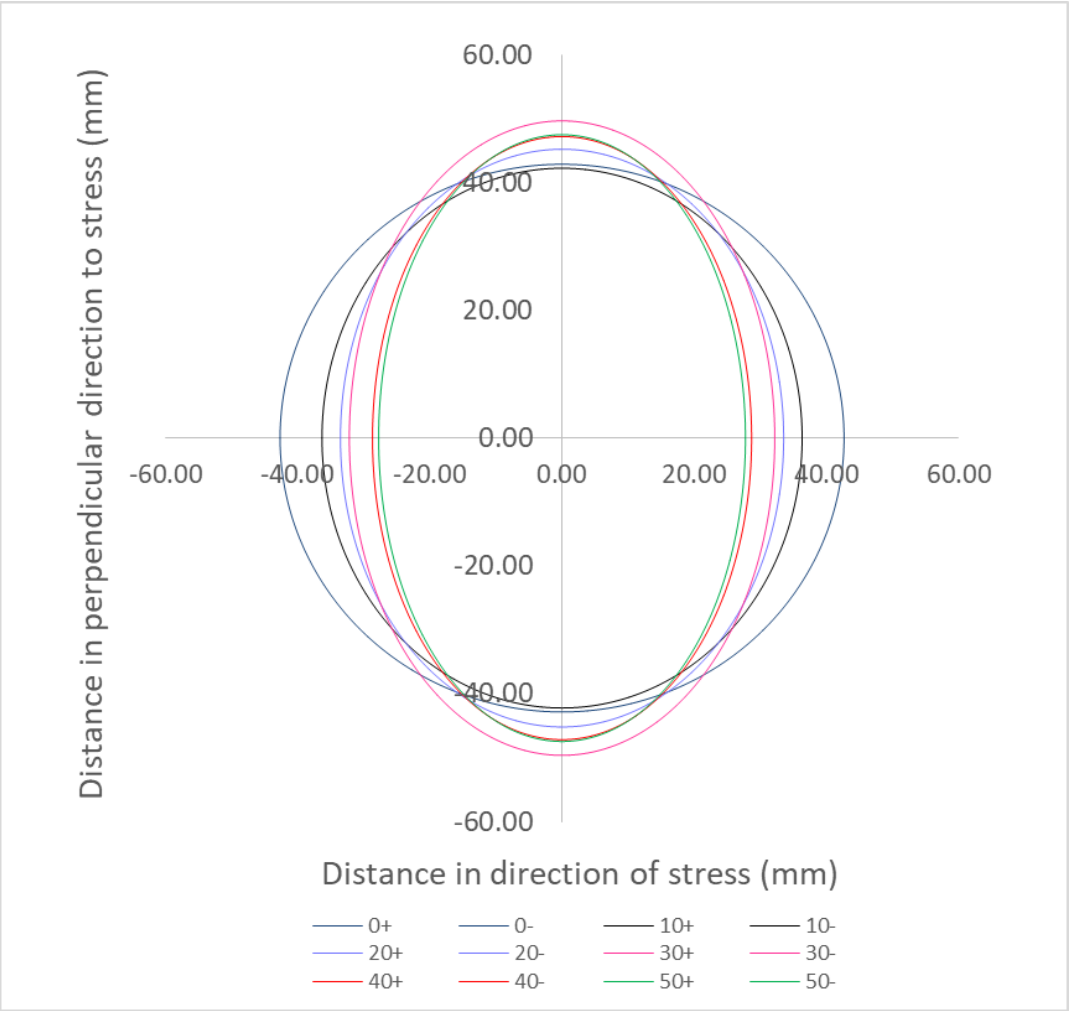

Figure 31. Cartesian coordinate of patterns immediately after release of stress.

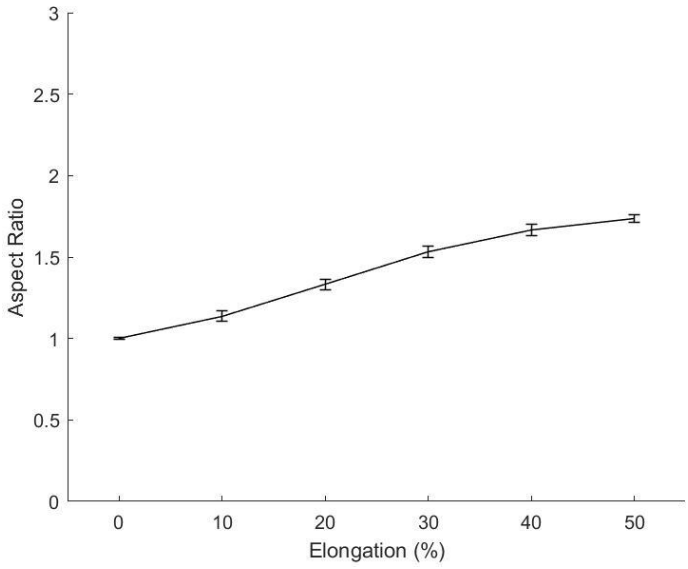

Figure 32. Aspect ratios of patterns obtained immediately after release. Data can be fit to equation $y = 0.0145x + 1.0649$, with R2 value of 0.995.

3.2.3. Liesegang patterns formed after release of mechanical stress

After releasing the mechanical stress, Liesegang patterns continued to form even when the stamp was removed from the hydrogel. However, in our experiments we kept the stamp on the hydrogel as long as the pattern monitoring continued. We named these rings formed after the release of the mechanical input as we named these as the “post rings”. We analyzed pattern formation (post-rings) 18 hours after releasing of mechanical stress, which is 42 hours in total (24 hours of stretching and 18 hours after releasing) from the beginning of experiment. We discovered an interesting fact after the analysis of the post rings: Post rings are precipitation patterns like Liesegang rings formed after releasing the stress and are formed mostly in the direction of applied stress. Therefore, we can say that post rings are the final set of rings that are not ‘completed’. Figure 33 shows the Liesegang patterns at different elongations after the release of mechanical stress. As illustrated in Figure 34, the number of post rings increases as elongation increases. This phenomenon can be explained by the change in concentration flux of outer electrolyte in hydrogel. When hydrogel is released from the mechanical stress, the distance in direction of applied stress will decrease and the distance in direction perpendicular to applied stress will increase. This will lead to increase in concentration flux of outer electrolyte in applied stress direction and decrease in perpendicular direction. This explains why post rings tend to form in stress direction rather than perpendicular direction since outer electrolyte ions tend to move in stress direction because of high flux. Moreover, as elongation increases, concentration flux in stress direction will increase too because distance will decrease much more. So, this explains why post rings form more as elongation increases, since there will be faster pattern formation when concentration flux of outer electrolyte is higher.

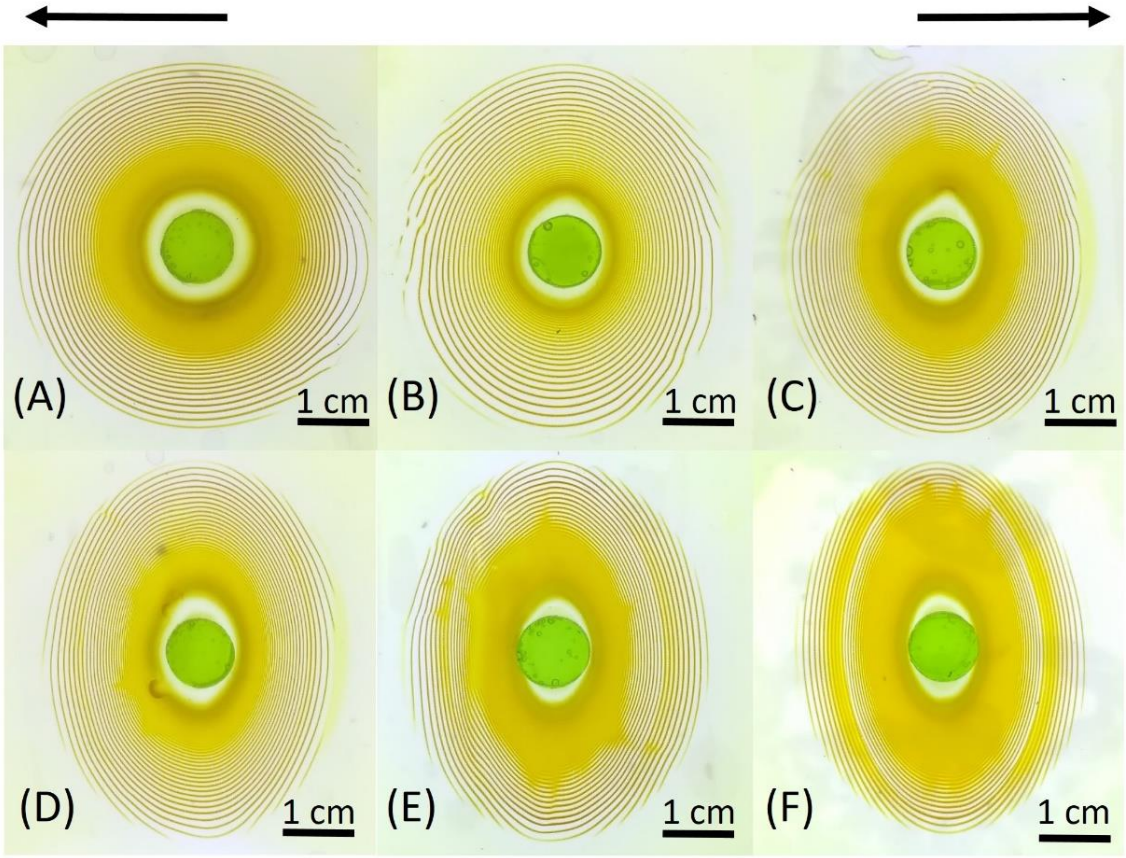

Figure 33. Patterns formed 18 hours (42 hours from the beginning) after release of the stress (Post rings). A) 0 % percentage elongation, B) 10 % percentage elongation, C) 20 % percentage elongation, D) 30 % percentage elongation, E) 40 % percentage elongation, F) 50 % percentage elongation. Arrows show the direction of applied mechanical stress. Concentrations of the components are as follows: inner electrolyte (chromate ion) = 0.01 M, outer electrolyte (copper (II) ion) = 1 M, acrylamide = 13.5 w%, BIS = 0.056 w%, KPS = 0.187 w%, TEMED = 0.0001 w%. T= 20 ˚C.

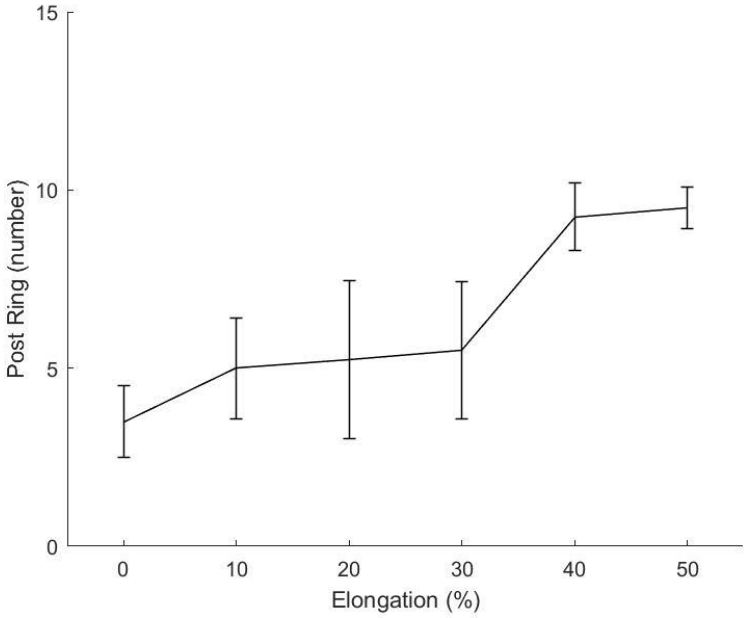

Figure 34. Number of post rings vs. percentage elongation.

3.2.4. Time lapse of Liesegang pattern formation

Liesegang patterns also obey time law as discussed in Section 1.1.2. Each band will form at particular time intervals. It is important to know how Liesegang pattern formation evolves with time when mechanical stress is applied to understand effect of mechanical stress completely. In Figure 35, LP formation as time passes is provided.

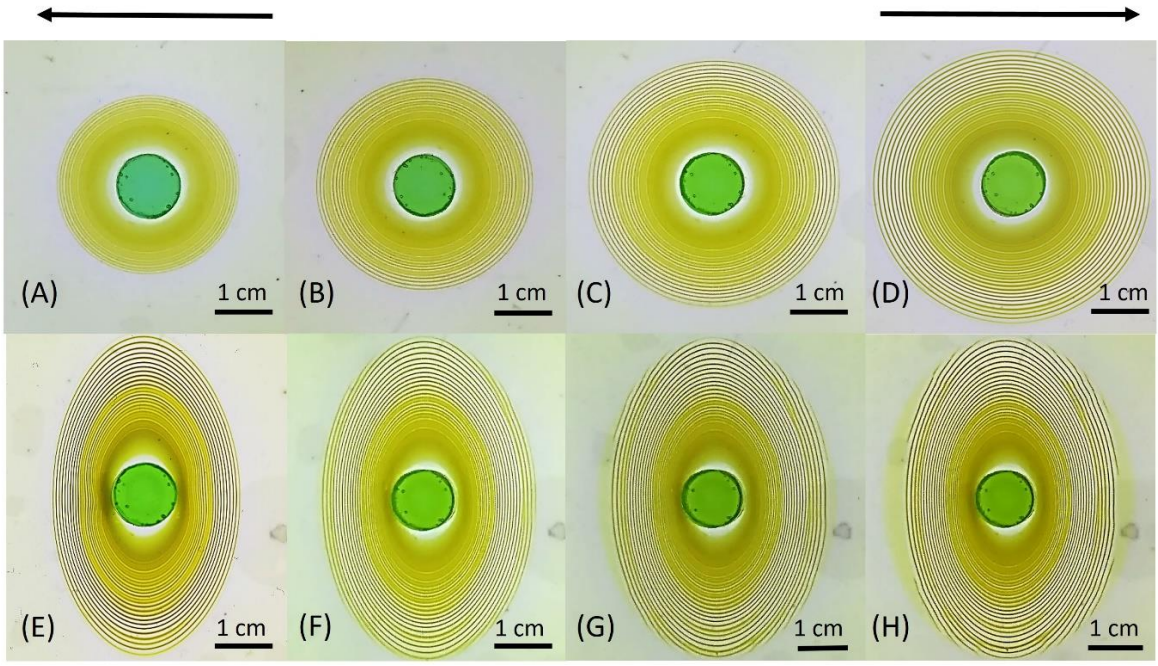

Figure 35. Time lapse of LP formation. A) after 6 hours (under stress), B) after 12 hours (under stress), C) after 18 hours (under stress), D) after 24 hours (under stress), E) after 24 hours (0 hours after released from stress), F) after 30 hours (6 hours after released from stress), G) after 36 hours (12 hours after released from stress), and H) after 42 hours (18 hours after released from stress). Arrows show the direction of applied mechanical stress. Concentrations of components as follows: inner electrolyte (chromate ion) = 0.01 M, outer electrolyte (copper (II) ion) = 1 M, acrylamide = 13.5 w%, BIS = 0.056 w%, KPS = 0.187 w%, TEMED = 0.0001 w%. T = 20 °C.

3.2.5. Potential applications

3.2.5.1. Local elastic deformation sensor

In section 1.1.5, we discussed that despite numerous studies conducted to understand Liesegang ring pattern formation, there is a little effort to make use of them in designing useful systems in material science. We believe that applying mechanical stress on hydrogels in reaction-diffusion systems will pave the way for designing a lot of crucial applications. One of the potential applications will be an elastic deformation sensor, which is discussed in section 1.2.2. In Figure 32, we

showed that how aspect ratio changes as elongation changes. In hypothetical system arranged in particular hydrogel that has defined inner and outer electrolytes, by only having a visual data and calculating aspect ratios after the elastic deformation will enable us to calculate the amount and direction of stress while elastic deformation cannot be easily determined by any other method. Furthermore, even local elastic deformation in the same sample can be determined by using our system. Figure 36 illustrates a setup in which local elastic deformation can be monitored. 5 stamps are placed in stretched hydrogel in different positions: one to center and others to the corners. We all know from material science perspective that in deformations, the areas close to the center will experience the highest stress. In Figure 36A, all of 5 different LPs have the same aspect ratio (which is 1 that shows they are perfect circles) and as we discussed before in section 3.2.1, stress will not change reaction-diffusion mechanism. However, Figure 36B proves that highest stress is exerted on the center of the sample since aspect ratio in the middle one is the highest, the one in the center has value of 2.366 while ones in the corners has values 1.638, 1.705, 1.766 and 1.677 which are pretty close to each other (has an average of 1.697±0.054). Aspect ratios of patterns in the corners are close to each other which proves that stress they experienced are the same which makes sense due of the their relative distances from the center are the same. Figure 36C shows the positions of the stamps in the Cartesian coordinate while it is released from the stress. Positions are given as the point for the centers of each stamp. The origin of the graph is the stamp in the center. It can be understood that relative positions of the stamps at the corners from the origin are close to each other (the averages of positions of the stamps in x and y directions are 23.09±1.58 and 15.53± 2.81 mm, respectively).

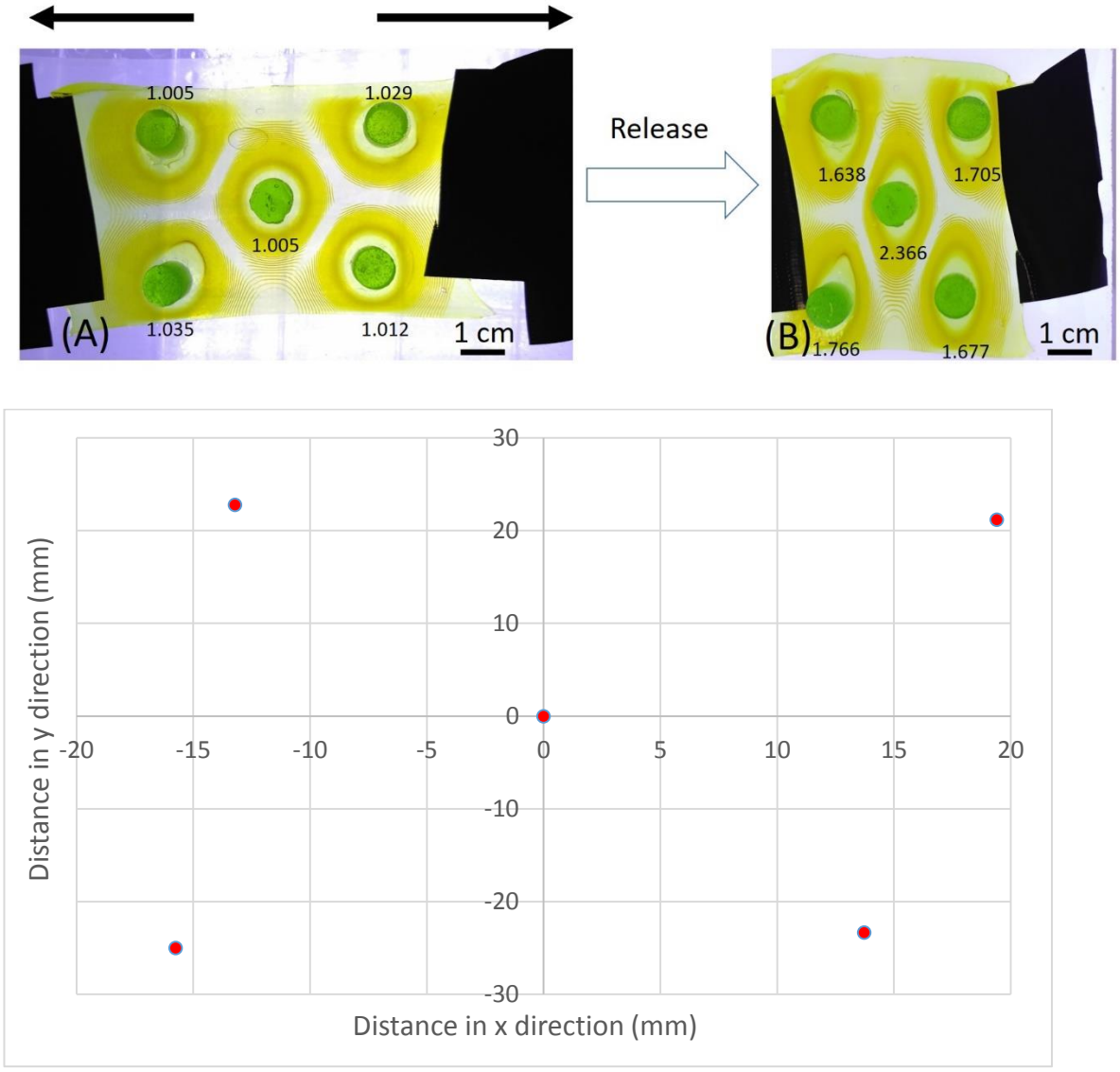

Figure 36. Setup for determining local elastic deformation by placing stamps to different positions. A) Pattern formation after 24 hours of applying stress, and B) immediate release of mechanical stress C) Positions of the stamps in the Cartesian coordinate while it is released from the stress (dots show the centers of the stamps and the origin is the stamp in the center. X direction is direction of applied stress and y direction is the perpendicular direction). Arrows show the direction of applied mechanical stress. Numbers shown on the stamps gives aspect ratios. Concentrations of components as follows: inner electrolyte (chromate ion) = 0.01 M, outer electrolyte (copper (II) ion) = 1 M, acrylamide = 13.5 w%, BIS = 0.056 w%, KPS = 0.187 w%, TEMED = 0.0001 w%. T = 20 ˚C.

3.2.5.2. History of deformation sensor

Another possible significant application of our system is to build an elastic deformation sensor that senses not only the direction and magnitude of mechanical stress, but also provides information about the exact time and duration, when the deformation took place. In Figure 37, time evolution of pattern formation is provided. LP patterns change geometrically, when mechanical stress is applied and released. So, by analyzing the shapes of bands and distances between the bands, we can distinguish the bands, which are formed during mechanical stress. By knowing the band number, which formed while stress is applied, the time when mechanical stress was applied can be calculated. It is a very good approach to record a history of elastic deformation, which is a totally novel application in elastic deformation sensors field. We designed a setup to demonstrate our idea: we applied a mechanical stress to hydrogel at first and after a particular time, we released the stress. Then, the sample stay released for that exact particular time, and sample stretched again. Consequently, we created a cycle of stress-release with the same intervals. In Figure 37, pattern formation in 2 cycles of stress-release with 3 hour interval (12 hours of the experiment in total) and in Figure 38, pattern formation in 3 cycles of stress-release with 2 hour interval (12 hours of the experiment in total) are shown. Elongation percentages were 40% for all stretching processes.

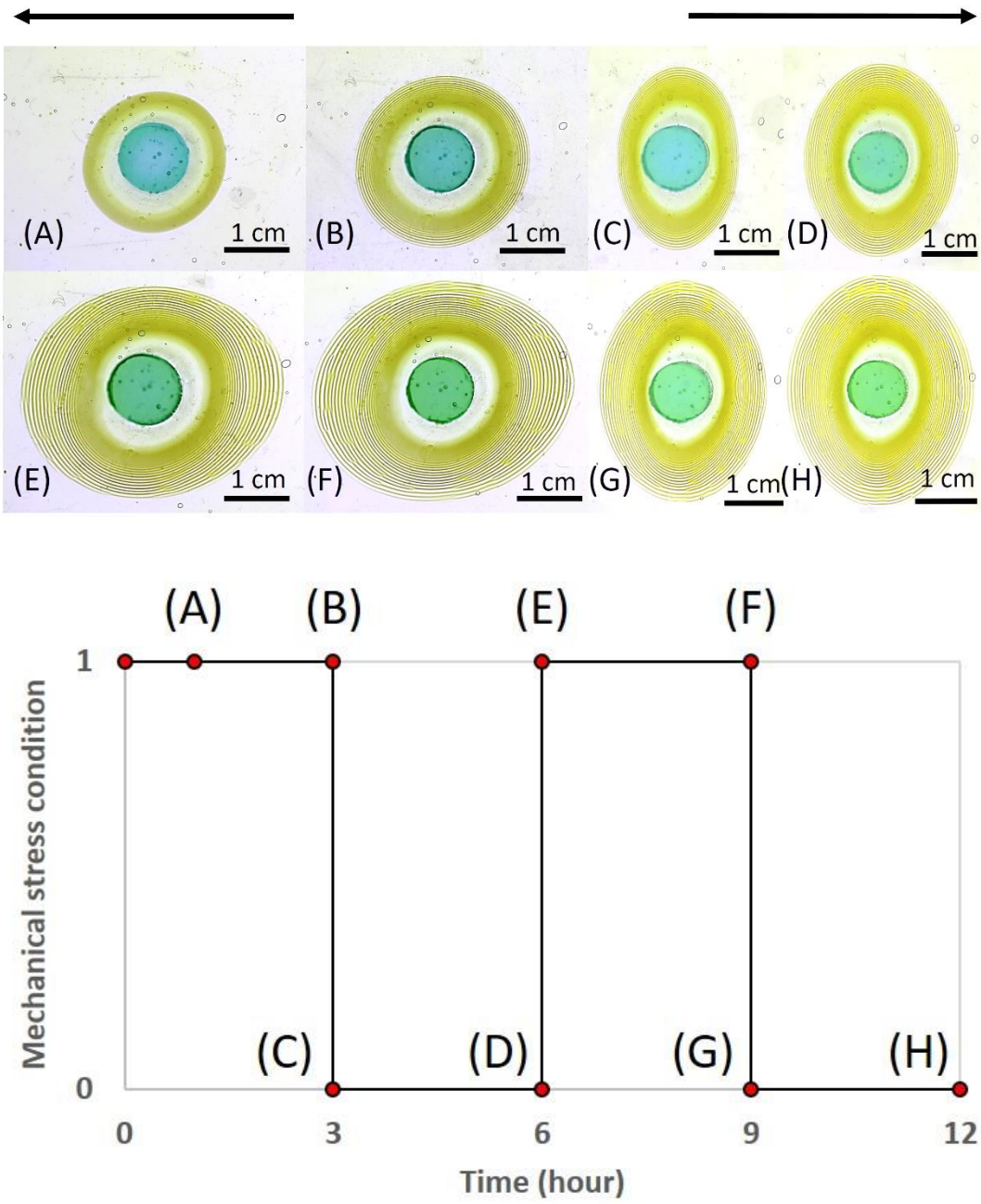

Figure 37. Pattern formation in 2 cycles of stress-release with 3 hour interval (12 hours of the experiment in total). A) after 1 hour (under stress), B) after 3 hours (under stress), C) after 3 hours (released from stress), D) after 6 hours (released from stress), E) after 6 hours (under stress), F) after 9 hours (under stress), G) after 9 hours (released from stress), H) after 12 hours (released from stress). Arrows show the direction of applied mechanical stress. If mechanical stress condition is 1, it means sample is under stress, and 0 means that there is no stress. Elongation percentage was 40%. Concentrations of components as follows: inner electrolyte (chromate ion)

= 0.01 M, outer electrolyte (copper (II) ion) = 1 M, acrylamide = 13.5 w%, BIS = 0.056 w%, KPS = 0.187 w%, TEMED = 0.0001 w%. T = 20 ˚C.

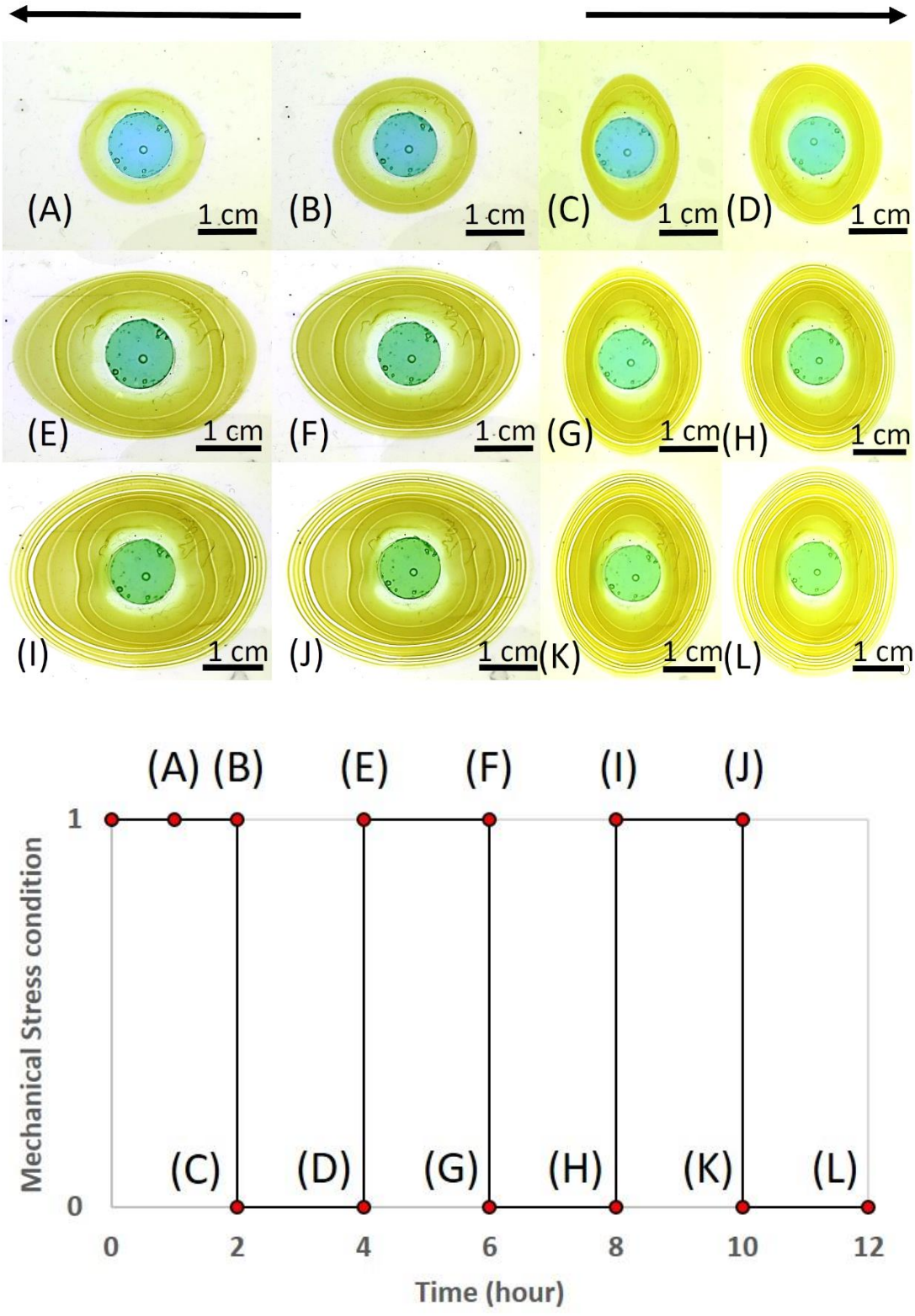

Figure 38. Pattern formation in 3 cycles of stress-release with 2 hour interval (12 hours of the experiment in total). A) after 1 hour (under stress), B) after 2 hours

(under stress), C) after 2 hours (released from stress), D) after 4 hours (released from stress), E) after 4 hours (under stress), F) after 6 hours (under stress), G) after 6 hours (released from stress), H) after 8 hours (released from stress), I) after 8 hour (under stress), J) after 10 hours (under stress), K) after 10 hours (released from stress), L) after 12 hours (released from stress). Arrows show the direction of applied mechanical stress. If mechanical stress condition is 1, it means sample is under stress, and 0 means that there is no stress. Elongation percentage was 40%. Concentrations of components as follows: inner electrolyte (chromate ion) = 0.01 M, outer electrolyte (copper (II) ion) = 1 M, acrylamide = 13.5 w%, BIS = 0.056 w%, KPS = 0.187 w%, TEMED = 0.0001 w%. T = 20 °C.

As seen in the above figures, the pattern formation in stress-release cycles are very different than the ones, which form under no stress or 'all-stressed' conditions. In Figure 39, comparison of the the final LPs before the release of the mechanical input, upon constant stress, stress-release cycle with 3 hour intervals and 2 hour intervals after 6 hours. At the first glimpse, it is observed that the samples, which are subject to cycles of stress-release show a distinct feature of ovality even when the final round of stress is not unloaded – in contrast to 'perfectly circular' constantly-stressed samples. This is largely because; when all samples are released, the 'post-rings' that form during the 'release-time' of the cycled samples appear as ovals (the aspect-ratio of which gets higher with higher number of release events) with long sides in the direction of stress, however, in the case for the constantly stressed samples the first and the only post-rings tend to be circular.

Under constant stress, all bands appear as perfect co-centric circles. On sample which is subjected to stress-release cycles of 3-hour intervals, interior bands (around 6 bands) that are close to stamp look like perfect circle, however the outer bands are ovals with long side horizontally (to the direction of stress). (Remember, previously under constant application of the stress, we obtained oval patterns one the stretching was released – however, these had their long side, in the perpendicular direction of stress after release (Figure 30). Finally, in the sample with stress-release cycles of 2-hour intervals, it is same as the one with cycles of 3-hour intervals but

having less number of initial bands that are perfect circles (2 bands) and the rest of the bands are oval with long side to the direction of stress. The reason why the sample with cycles of 3-hour intervals has more number of initial 'perfect circle' bands is obvious: It has more time to develop these circles until stress is released, so more rings will form while it is stretched for the first time. Thus, this setup not only perfectly shows if there are stress-release cycles, also it shows exact time of cycles. This setup can record history of deformation. It is the first time in literature such an application regarding elastic deformation sensors has been developed.

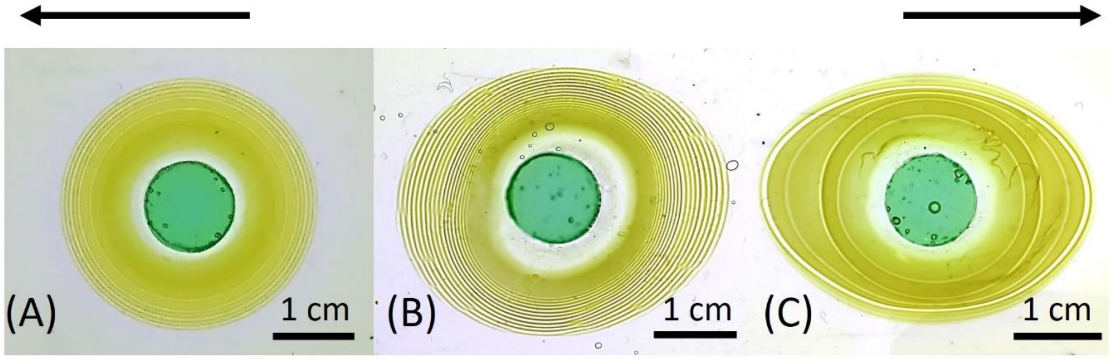

Figure 39. Comparison of different stress-release cycle with different time intervals after 6 hours while stretched. A) at constant stress, B) with 3 hour interval, C) with 2 hour interval. Arrows show the direction of applied mechanical stress. Elongation percentages were 40% for all of them.

If we look closer into the patterns, we see that not only the shape of patterns are changing, also distances between bands are changing too. Compare the LPs formed at the constant stress, cycles with 3-hour intervals and cycles with 2-hour intervals, respectively in Figure 40, 41, and 42. In constant stress one, the band distance increases in geometric series and there is no large and sudden increase or decrease between bands. However, in 3 hour interval sample, there is a sudden increase in distance in the border of line 2 to 3 (change from without stress to under stress). It is more obvious in 2-hour interval sample. Notice the large increase in the borders of line 2 and 3 and line 4 and 5 (both of them are changes from without stress to under stress). These increases in the distances after applying stress can be attributed to the

fact that when hydrogel is stretched, distance in stretching direction will increase and it will lead to the decrease in the concentration gradient of outer electrolyte and thus decrease in diffusion flux of outer electrolyte. Consequently, this will lead to formation of next pattern at a farther distance since supersaturation level of outer electrolyte will be reached at a farther distance due to the decrease in diffusion flux of outer electrolyte. This change in the distances not only shows whether there is a change in the magnitude and direction of mechanical input, but also shows the exact time when the change happened since we know in which bands there is an increase in distance and this gives information about time. Although here shown with only qualitative analysis, these changes are quite obvious to human eye, which straightforwardly gives an idea of how, when and for how long the deformation has taken place in the sample. We are currently developing an analytical tool to analyze the deformation in samples digitally, too.

Figure 40. Pattern formation with a constant stress for 12 hours and released in the end. Caption is taken from direction of applied stress. Elongation percentage was 40%.

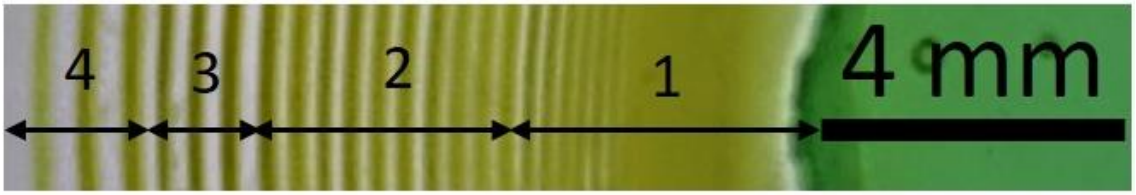

Figure 41. Qualitative analysis of pattern formation with a 2 cycle of stress-release with 3 hour interval for 12 hours (without stress in the final case). Caption is taken from direction of applied stress. Line 1 corresponds to 0-3 hours under stress, line 2 to 3-6 hours without stress, line 3 to 6-9 hours under stress, line 4 to 9-12 hours without stress. Elongation percentage was 40%.

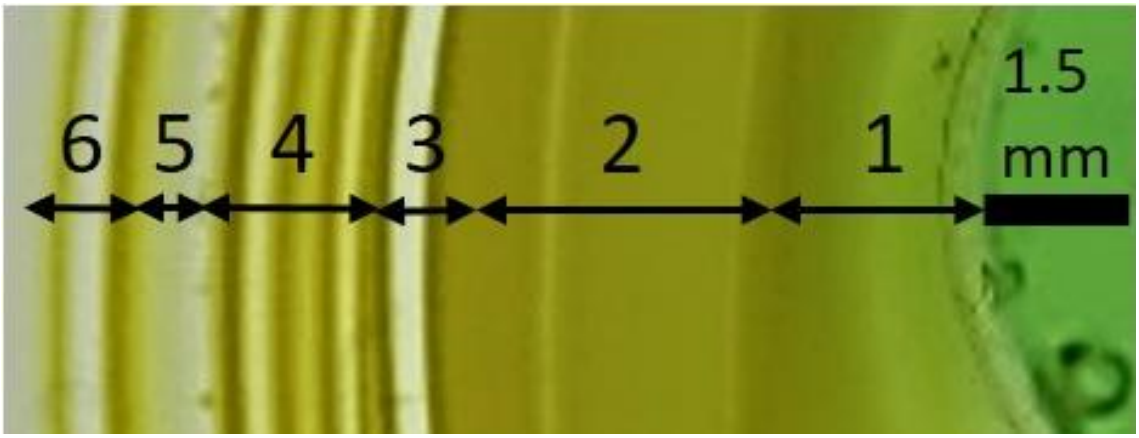

Figure 42. Qualitative analysis of pattern formation with a 3 cycle of stress-release with 2 hour interval for 12 hours (without stress in the final case). Caption is taken from direction of applied stress. Line 1 corresponds to 0-2 hours under stress, line 2 to 2-4 hours without stress, line 3 to 4-6 hours under stress, line 4 to 6-8 hours without stress, line 5 to 8-10 hours under stress, and line 6 to 10-12 hours without stress. Elongation percentage was 40%.

CHAPTER 4

4 CONCLUSION

In this thesis, we showed that pattern formation governed by reaction-diffusion systems can be controlled and engineered by changing chemical composition and applying mechanical stress. For this purpose, in the first part, we synthesized polyacrylamide-alginate hybrid hydrogel and poly-N,N'-dimethylacrylamide hydrogels and formed precipitation patterns of magnesium hydroxide precipitate in them. Then by changing chemical composition of the system including inner and outer electrolyte, acrylamide, DMMA and alginate concentration, we showed that starting and finishing distances of precipitation patterns change. Furthermore, we applied mechanical stress on hydrogel medium to show that mechanical stress change pattern shapes from circular rings to oval shapes when stress is released. Ovality and aspect ratio of patterns increase as elongation increases and radius of pattern in the applied stress direction decreases.

In second part, Liesegang patterns are produced in polyacrylamide hydrogel for investigation of the effect of mechanical stress. It was shown that applying mechanical stress on gel medium does not change reaction-diffusion mechanism – the changes in the formed pattern are only due to the geometry change of the gel. We demonstrated that, upon release of the mechanical stress, the radius of the last ring decreases in the applied stress direction and increases in the perpendicular direction. Aspect ratio increases linearly with increase of elongation. Furthermore, we discovered "post rings" are formed after the release of mechanical stress, appearing mostly in the direction of applied stress. The number of the post rings increase as elongation increases, presumably due to an increase of concentration flux of outer electrolyte because of distance drop in the stress direction after release.

Finally, we also show some preliminary result in the direction of potential applications of our results. We showed a simple elastic deformation sensor that can map the stress in the hydrogel sample using the aspect ratio of the multiple LP patterns on the sample. Finally, we showed a primitive but unprecedented example of direction, magnitude, time and duration sensor for elastic deformation in hydrogels.

We hope that our results help the fundamental understanding of these artistic patterns also found in nature, which currently by itself is an enigma. With these, we also hope that we provide the spark for some new applications using these systems, which can be practical and useful in the end.

REFERENCES

1. E. Nakouzi, O. Steinbock. (2016). Self-organization in precipitation reactions far from the equilibrium, Sci. Adv. 2:e1601144
2. S. Sadek, R. Sultan. (2010). In Precipitation Patterns in Reaction-Diffusion Systems, Lagzi, I. Ed.; Research Signpost: Trivandrum, p 1-43
3. R. E. Liesegang. (1896). Ueber einige eigenschaften von gallerten. Naturw. Wochenschr. 10, 353–362
4. L. Badr, Z. Moussa, A. Hariri, R. Sultan. (2011). Band, target, and onion patterns in Co(OH)2 Liesegang systems. Phys. Rev. E 83, 016109
5. I. Lagzi. (2012). Controlling and engineering precipitation patterns. Langmuir 28, 3350–3354
6. R. F. Sultan, Abdel-Fattah, M. Abdel-Rahman. (2013). On dynamic self-organization: Examples from magmatic and other geochemical systems. Lat. Am. J. Solids Struct. 10, 59–73
7. M. C. K. Jabłczyński. (1923). La formation rythmique des précipités: Les anneaux de Liesegang. Bull. Soc. Chim. France 33, 1592–1603
8. R. Matalon, A. Packter. (1955). The Liesegang phenomenon. I. Sol protection and diffusion. J. Colloid Sci. 10, 46–62
9. H. W. Morse, G. W. Pierce. (1903). Diffusion and supersaturation in gelatine. Phys. Rev. 17, 129
10. B. A. Grzybowski. (2009). Chemistry in Motion: Reaction–Diffusion Systems for Micro- and Nanotechnology, John Wiley and Sons, Chichester, UK
11. R. Sultan, R. Halabieh. (2000). Effect of an electric field on propagating Co(OH)2 Liesegang patterns. Chem. Phys. Lett. 332, 331–338
12. T. Karam, R. Sultan. (2013). Effect of an alternating current electric field on Co(OH)2 periodic precipitation, Chemical Physics 412, 7-12
13. Y. Kanazawa, Y. Asakuma. (2014). Periodic Precipitation of Liesegang System under Microwave Radiation, J. Chem. Chem. Eng. 8, 331-334
14. R. Makki, M. Al-Ghoul, R. Sultan. (2009). Propagating Fronts in Thin Tubes: Concentration, Electric, and pH Effects in a Two-Dimensional Precipitation Pulse System, J. Phys. Chem. A 113, 6049–6057
15. L. Badr, R. Sultan. (2009). Ring Morphology and pH Effects in 2D and 1D Co(OH)2 Liesegang Systems, J. Phys. Chem. A 113, 6581-6586

16. I. T. Bensemann, M. Fialkowski, B. A. Grzybowski. (2005). Wet stamping of microscale periodic precipitation patterns. J. Phys. Chem. B 109, 2774–2778
17. H. Yan, Y. Zhao, C. Qiu, H. Wu. (2008). Micropatterning of inorganic precipitations in hydrogels with soft lithography, Sensors and Actuators B 132, 20-25
18. M. C. Koetting. J. T. Peters, S. D. Steichen, N. A. Peppas. (2015). Stimulus-responsive hydrogels: Theory, modern advances, and applications, Materials Science and Engineering R 93, 1-49
19. Y.H. Bae, T. Okano, S.W. Kim. (1990). Temperature dependence of swelling of crosslinked poly(N,N'-alkyl substituted acrylamides) in water, J. Polym. Sci. B: Polym. Phys. 28, 923-936
20. P. Gupta, K. Vermani, S. Garg. (2002). Hydrogels: from controlled release to pH-responsive drug delivery, Drug Discov. Today. 7, 569-79
21. Q. Wu, L. Wang, H. Yu, J. Wang, Z. Chen. (2011). Organization of Glucose-Responsive Systems and Their Properties, Chem. Rev. 111, 7855–7875
22. V.V. Ramanan, J.S. Katz, M. Guvendiren, E.R. Cohen, R.A. Marklein, J.A. Burdick. (2010). Photocleavable side groups to spatially alter hydrogel properties and cellular interactions, J. Mater. Chem. 20, 8920
23. Z. Liu, P. Calvert. (2000). Multilayer Hydrogels as Muscle-Like Actuators, Adv. Mater. 12, 288-291
24. J.Y. Sun, X. Zhao, W.R.K. Illerperuma, O. Chaudhuri, K.H. Oh, D.J. Mooney, J.J. Vlassak, Z. Suo. (2012). Highly stretchable and tough hydrogels, Nature
25. Y. J. Liu, W. T. Cao, M. G. Ma, P. Wan. (2017). Ultrasensitive Wearable Soft Strain Sensors of Conductive, Self-healing, and Elastic Hydrogels with Synergistic "Soft and Hard" Hybrid Networks, ACS Appl. Mater. Interfaces, 9, 25559−25570
26. G. Cai, J. Wang, K. Qian, J. Chen, S. Li, P. S. Lee. (2017). Extremely Stretchable Strain Sensors Based on Conductive Self-Healing Dynamic Cross-Links Hydrogels for Human-Motion Detection, Adv. Sci., 4, 1600190